

Manuscript Number:

Title: Peak shaving strategy through a Solar Combined Cooling and Power system in remote hot climate areas

Article Type: Original Paper

Keywords: combined cooling and power; Integrated Solar Combined Cycle; Concentrating Solar Power; absorption chiller; peak demand.

Corresponding Author: Dr. Silvia Ravelli,

Corresponding Author's Institution: University of Bergamo

First Author: Antonio Perdichizzi

Order of Authors: Antonio Perdichizzi; Giovanna Barigozzi; Giuseppe Franchini; Silvia Ravelli

Abstract: An effective combination of district cooling with electric power production in an integrated solar combined cycle is presented and evaluated. A remote area in hot climate is assumed as location to highlight the importance of peak shaving strategy in an isolated or weakly interconnected power system. Two solutions for handling peak power demand are taken into account in the present investigation. On the one hand, the integration of a Concentrated Solar Power system (CSP) with a combined cycle power plant is considered to match peak power demand on the grid. On the other hand, the adoption of a district cooling system where cooling energy is produced by absorption chillers is proposed, instead of mechanical refrigeration, to reduce and flatten the load profile.

The case study refers to a combined cycle (CC) based on a 46 MW Siemens SGT-800 gas turbine. The CC plant is integrated with a Parabolic Trough Collectors (PTC) solar field and double-effect steam driven absorption chillers feeding a district cooling network. The solar combined cooling and power (SCCP) system is designed to operate in "island mode" to match both electrical and cooling demand on an hourly basis, on a typical winter and summer day. A modeling procedure is applied to accurately simulate the plant operation, including off-design behavior of all plant components. During the day the solar source has the highest priority, whilst the gas turbine (GT) is operated at part-load to follow the load profile.

Electric efficiency and fuel savings for the SCCP plant are computed and compared against the ones resulting from a conventional pure fossil system based on analogous combined cycle and compression refrigeration units. Results show that a SCCP system can significantly reduce fossil fuel consumption in both summer and winter peak hours, while providing higher overall efficiency through the whole day, both in summer and winter.


Dear Editor,

please consider that my co-authors and I intend to submit the present manuscript to Applied Energy. This manuscript has not been previously published in another journal.

Here follows a brief summary:

The present case study refers to a combined cycle integrated with a parabolic trough collector solar field and double-effect steam driven absorption chillers. The solar combined cooling and power system is designed to operate in “island mode” to match both electrical and cooling demand on an hourly basis, for typical winter and summer days. A modeling procedure is applied to accurately simulate the system operation in off-design conditions. Electric efficiency and fuel consumption are computed and compared against the ones resulting from a conventional “pure fossil” system based on a combined cycle and compression refrigeration units.

The corresponding author

X 
Silvia Ravelli

Silvia Ravelli
Assistant Professor
Department of Engineering
University of Bergamo
5 Marconi St
24044 Dalmine (BG)
Phone +39 035 2052346
Fax +39 035 2052077
e-mail: silvia.ravelli@unibg.it

Highlights

- A solar combined cooling and power (SCCP) system is simulated in island mode
- The case study refers to a combined cycle with solar field and absorption chillers
- Electrical and cooling demand are matched for typical winter and summer days
- The SCCP system has higher efficiency than a conventional pure fossil plant
- Another advantage of the SCCP system is the reduction in fossil fuel use

Peak shaving strategy through a Solar Combined Cooling and Power system in remote hot climate areas.

A. Perdichizzi, G. Barigozzi, G. Franchini, S. Ravelli*

Department of Engineering, Bergamo University, 24044 Dalmine, Italy

Abstract

An effective combination of district cooling with electric power production in an integrated solar combined cycle is presented and evaluated. A remote area in hot climate is assumed as location to highlight the importance of peak shaving strategy in an isolated or weakly interconnected power system. Two solutions for handling peak power demand are taken into account in the present investigation. On the one hand, the integration of a Concentrated Solar Power system (CSP) with a combined cycle power plant is considered to match peak power demand on the grid. On the other hand, the adoption of a district cooling system where cooling energy is produced by absorption chillers is proposed, instead of mechanical refrigeration, to reduce and flatten the load profile.

The case study refers to a combined cycle (CC) based on a 46 MW Siemens SGT-800 gas turbine. The CC plant is integrated with a Parabolic Trough Collectors (PTC) solar field and double-effect steam driven absorption chillers feeding a district cooling network. The solar combined cooling and power (SCCP) system is designed to operate in “island mode” to match both electrical and cooling demand on an hourly basis, on a typical winter and summer day. A modeling procedure is applied to accurately simulate the plant operation, including off-design behavior of all plant components. During the day the solar source has the highest priority, whilst the gas turbine (GT) is operated at part-load to follow the load profile.

Electric efficiency and fuel savings for the SCCP plant are computed and compared against the ones resulting from a conventional pure fossil system based on analogous combined cycle and compression refrigeration units. Results show that a SCCP system can significantly reduce fossil fuel consumption in both summer and winter peak hours, while providing higher overall efficiency through the whole day, both in summer and winter.

Keywords: combined cooling and power; Integrated Solar Combined Cycle; Concentrating Solar Power; absorption chiller; peak demand.

Nomenclature

<i>ABS</i>	absorption chiller
<i>CC</i>	combined cycle
<i>COMP</i>	compression chiller
<i>COP</i>	coefficient of performance

* Corresponding author. Tel.: +39 035 2052346; fax: +39 035 2052077
E-mail address: silvia.ravelli@unibg.it (S. Ravelli).

30	<i>DNI</i>	direct normal irradiation, W/m ²
31	<i>ECO</i>	economizer
32	<i>EVA</i>	evaporator
33	<i>GT</i>	gas turbine
34	<i>HP</i>	high pressure
35	<i>HTF</i>	heat transfer fluid
36	<i>I_b</i>	beam radiation, degrees
37	<i>K</i>	incident angle modifier
38	<i>ISCC</i>	integrated solar combined cycle
39	<i>LHV</i>	low heating value, kJ/kg
40	<i>LP</i>	low pressure
41	<i>m_{fuel}</i>	fuel mass flow rate, kg/s
42	<i>P_{el}</i>	electric power, MW
43	<i>P_{th}</i>	thermal power, MW
44	<i>PTC</i>	parabolic trough collector
45	<i>SCCP</i>	solar combined cooling and power (plant)
46	<i>SH</i>	superheater
47	<i>ST</i>	steam turbine
48	<i>T</i>	temperature, K
49	<i>η</i>	efficiency, %

50

51 **1. Introduction**

52 Public awareness of the need to reduce global warming and significant increase in the prices of conventional energy
53 sources have encouraged many countries to promote renewable energy applications. Such renewable energy sources,
54 like solar or wind, have potential for increasing use in the next years. Actually, the integration of these renewable
55 energy sources into fossil fuel systems can provide a more economic, environment friendly and reliable supply of
56 electricity, whatever the load demand, as compared to single-use of such systems. However, some issues need to be
57 faced. Firstly, hybrid systems require not only optimal sizing to meet the load requirements [1] while minimizing
58 investment and capital costs, but also advanced control tools to assure safe operation [2]. Secondly, to achieve
59 commercialization and widespread use, an efficient energy management strategy needs to be implemented. In the
60 published literature there are several contributions discussing technical, economic and environmental issues related to

possible scenarios of the penetration of renewable sources for energy generation, at international, national and local levels, as reported in [3].

The present work was intended to contribute to the process of identification of new solutions for the transition from a “fossil-fuel-based” energy generation system to a smart “renewable-based” scenario. A remote area in hot climate was assumed as location. Accordingly, the opportunity to integrate solar power into an isolated or weakly interconnected power system, based on a combined cycle, and the problem of summer peaking electricity demand due to air conditioning were both addressed in this study. The resulting scenario fits well with the current situation in the Middle East countries. For example, efforts by Saudi Electricity Company SEC in the Kingdom of Saudi Arabia to meet the mounting demand during peak times are reported in [4]. In the same geographic context, an extensive review of the various gas turbine inlet cooling technology options was provided by Al-Ibrahim and Varnham [5]. Methods of increasing the energy contribution from existing gas turbine plants through inlet air cooling can make a substantial contribution to the summer peak demand for electric power which almost doubles the off-peak demand in Saudi Arabia. Another example is provided by Ameri et al. [6]. They focused on gas turbines coping with the peak electricity demand in Iran. The use of thermal energy storage for gas turbine inlet cooling was studied to increase the gas turbine peaking capacity during operation in hot weather. Similarly a study of capacity enhancement of the Chabahar (in the south of Iran) gas turbine installation using an absorption chiller was performed by Ameri and Hejazi [7].

Also, examples of hybrid systems including solar power and air conditioning are documented in literature as specific case studies. Reference [8] assumed that the base load demand (in the state of Victoria, Australia) is supplied by conventional base load generators, with solar power generators able to supply up to 4,500 MW electrical maximum in day time. The analysis demonstrates that matching the daytime demand profile with the corresponding instant solar power supply profile may help reducing peak demands and their prices. Existing experiences and realizations of PTC in solar cooling systems are summarized in [9], as well as survey of PTC potential application in feeding double effect absorption chillers. The different solar cooling technologies are discussed in [10] in view of the potential to reduce the electricity consumptions. Solar thermal with single-effect absorption system resulted in the best option. Calise [11] developed a dynamic model of a solar heating and cooling system based on the coupling of PTC with a double-stage LiBr–H₂O absorption chiller; auxiliary energy for both heating and cooling is supplied by a biomass-fired heater. System performance is computed for seven Mediterranean cities in Italy, Spain, Egypt, France, Greece and Turkey. As expected, the economic profitability is higher for the hottest climates.

Another smart use of solar energy was studied by Palenzuela et al. [12]. They evaluated different alternatives for the integration of desalination technologies in the cooling of CSP plants in the Mediterranean area, where fresh water shortage coexists with high solar radiation. Simulation results showed that the integration of a thermal vapor

92 compression multi-effect distillation plant into a CSP plant is more competitive than each plant independently. The
93 coupling is more efficient thermodynamically and also more economic than the decoupling, since it requires a smaller
94 solar field for the same power and water production.

95 Recently, the concept of smart grid has been successfully applied to the electric power systems with the aim of
96 integrating renewable energy sources into power system grids. A review of work done in renewable smart grid systems
97 across the globe indicates the promising potential of such research characteristics in the future [13]. On the other hand,
98 the great challenges posed by integration of large amounts of renewable resources to both planning and operation of
99 modern electric infrastructures are discussed by Wang et al. [14]. Abdullah et al. [15] pointed out that the integration of
100 renewable generation has impacts on the energy supply and service continuation of the distribution networks, because
101 of the time varying demand and the uncertainty in power generation from renewable energy. Demand side response
102 (DSR) models such as the one presented in [16, 17] assist electricity consumers from peak to off-peak demand periods
103 averting congestion on the electrical network. This is expected to enable consumers to be engaged in mitigating peak
104 demands on the electricity network and make improved utilization of the electricity infrastructure. Additionally, the
105 scheme enables commercial and industrial consumers to achieve immediate financial savings. For residential consumers
106 on flat-rate tariffs it secures financial benefits by reducing energy consumptions at peak-demand periods. Demand side
107 management will be a key component of future smart grid that can help reduce peak load and adapt elastic demand to
108 fluctuating generations.

109 Focusing on the above mentioned Middle East countries, and particularly on the Gulf region, most of the power demand
110 in summer days is due to cooling energy for air conditioning. This makes the electrical grid undergo huge load
111 variations not only between summer and winter days, but even during a single summer day. In an isolated or weakly
112 interconnected grid, a power plant (i.e. a combined cycle) is planned to match peak demand. Therefore it is forced to
113 work in heavy off-design conditions for most of the time, thus causing significant efficiency penalties and larger fuel
114 consumptions. The adoption of a district cooling system where cooling energy is produced by absorption chillers,
115 instead of mechanical refrigeration, can lead to a significant lowering and flattening of the load profile. Another
116 solution to efficiently match peak power demand on the grid is the integration of a CSP system with a power plant. Both
117 solutions, if integrated in a unique system, are expected to reduce the size of the power plant thus allowing for more
118 stable off-design operating conditions and higher efficiency. To quantify these beneficial effects, an Integrated Solar
119 Combined Cycle (ISCC) with steam extraction to operate double-effect absorption chillers was compared against the
120 conventional fossil-fuel solution, i.e combined cycle (CC) with compressor refrigeration, in terms of global efficiency
121 and load-following capability. This approach is somewhat different from that used in the published literature. In fact
122 previous studies on gas turbine systems with combined heat, power and absorption refrigeration demonstrated the

technical and economic feasibility of different plant solutions (single, double or triple absorption chillers fed by waste heat exhausted from a gas turbine in [20]; three double-effect absorption chillers fed by waste heat from a combined cycle in [21]). Then exergy/energy balances for a gas turbine trigeneration system and its components are presented in [22]. A trigeneration system, consisting of a gas turbine cycle, a steam turbine cycle and a single-effect absorption chiller, was assessed from an environmental point of view by Ahmadi et al. (2011): results indicated that the carbon dioxide emissions are less than those for the compared systems. In all these works, the trigeneration system performance was evaluated according to different layouts, at design conditions and constant overall efficiency. Load following mode of operation was not implemented. Conversely, the demonstrated capability of the SCCP plant to follow daily variations of the power demand is the added value of the present investigation. Moreover, off design performance of plant components under real operating conditions is carefully evaluated.

133

134 **2. System configuration**

135 The power system is assumed to be isolated and conceived for a mid-size community (roughly around 50,000
136 inhabitants). Daily patterns of power and cooling demand are defined for a typical summer (Fig. 1) and winter day (Fig.
137 2). Daily patterns are determined by processing published data of the Regulation & Supervision Bureau of the Abu
138 Dhabi Emirate. The peak power results to be 83 MW in summer, and only 42 MW in winter. It can be seen that there is
139 a big variation in the power request between day and night: about 50% in summer and 40% in winter. Furthermore,
140 about 45% of the total electricity demand in summer is due to chiller consumptions, while only 15-20% in winter. To
141 mitigate these large load variations, the two above mentioned options, i.e. absorption chillers and CSP, have been
142 considered in the SCCP plant.

143 **2.1. Layout of the SCCP plant**

144 The power plant configuration assumed for the present analysis is shown in Fig. 3. It is based on a combined cycle
145 integrated with a PTC solar field and two-stage absorption chillers. The gas turbine cycle is combined with a steam-
146 driven regenerative bottoming cycle to boost power production and cycle efficiency. Exhaust heat from the gas turbine
147 generates high pressure steam in a dual pressure heat recovery steam generator (HRSG). Steam is then introduced in the
148 bottoming Rankine cycle. Steam from the solar field is also fed to the Rankine cycle to increase power production in the
149 sunny hours. Low pressure steam is then extracted from the steam cycle to drive absorption chillers for cooling
150 generation. The condensate flow from the absorption chiller returns to the Rankine cycle. Design and off design
151 characteristics of the major SCCP plant components are reported here below together with those of the conventional
152 fossil fuel CC, assuring the peak power coverage.

153

154 2.2. ISCC

155 An integrated solar combined cycle system combines a solar field and a gas fired CC power plant. The steam generated
156 by the solar section is joined to the one produced in the HRSG and expanded in the steam turbine. A large part of the
157 steam cycle is shared with the solar section and remains almost unchanged. Steam turbine and condenser over sizing is
158 anywhere needed to accommodate solar steam.

159 CC design parameters in fossil fuel operation are shown in Table 1. The CC plant includes a Siemens SGT-800 gas
160 turbine rated 46.4 MWe at ISO conditions (Fig. 4). The steam section is based on a dual pressure HRSG generating
161 steam at 69 bar and 7.7 bar. Steam is then expanded in a steam turbine producing 20.8 MWe. HRSG heat transfer
162 sections were sized assuming an approach point of 26°C and pinch point temperature difference values of 9°C and 8°C
163 for HP and LP evaporator, respectively. Turbine efficiency values of 83% and 87.5% were set for HP and LP steam
164 turbine sections. An air cooled condenser with a design pressure of 0.06 bar at ISO conditions was considered.

165 In the ISCC plant, a 150,000 m² parabolic trough solar field was considered. Synthetic oil (Therminol VP-1) was
166 assumed as heat transfer fluid (HTF). Constant HTF temperature values of 292°C and 392°C were set at the solar field
167 inlet and outlet. The thermal energy from the solar field is transferred to the bottoming cycle by means of a heat
168 exchanger HX (Fig. 4) including an economizer, an evaporator and a superheater. HX receives preheated feedwater
169 drawn from the HRSG and returns superheated steam. This mixes with the steam exiting the HP evaporator and the
170 resulting flow rate is sent to the HP superheater. Note that the feedwater extraction point was assumed downstream of
171 the first stage (ECOHP1). This turned out to be the best effective integration of the solar thermal input into the CC,
172 allowing the whole steam flow rate to be superheated to the design temperature value (i.e. 522°C). HX was designed to
173 receive the highest oil flow rate occurring in the summer day. With a design pinch and approach of 5°C and 10°C, the
174 resulting design value of the solar steam flow rate is 32.3 kg/s, at 95.3 bar and 385.2°C. As a result, the ISCC net power
175 production grows to 94.3 MW (Table 2). Fig. 5 shows the T-Q diagram at design condition.

176 With respect to the pure fossil CC scheme, the following steam power block components were modified to admit the
177 solar steam:

- 178 - HP and LP turbine: the design point was set at the maximum turbine inlet steam flow rate (solar + fossil) that can be
179 produced in the summer day.
- 180 - HP superheater: the surface was increased to get the desired steam temperature (522°C) for the largest inlet steam
181 flow.
- 182 - Condenser: it was designed to handle the whole additional steam flow while maintaining the turbine design
183 backpressure (0.06 bar) at ISO condition.

184 A solar dispatching strategy was adopted, so no auxiliary burner or thermal storage system was required.

Concerning the HP steam turbine control, sliding pressure condition was assumed. GT off-design operation was considered depending on ambient temperature and humidity. Model predictions were checked against performance data declared by manufacturer. Fig. 6. shows that the developed GT model provides a good correspondence between simulated and declared power output. GT control too was performed consistently with the one adopted by manufacturer (Fig. 7). For a load factor ranging from 100% down to 70%, air mass flow rate is reduced by progressively closing inlet guide vanes (IGV), while turbine firing temperature is maintained at the nominal value. The resulting exhaust temperature increases while reducing the load factor. For still lower load factors, IGV opening remains at the minimum value, giving a constant airflow, while turbine firing temperature is progressively reduced. The turbine outlet temperature decreases as well, with a penalty on exhaust heat recovery.

2.3. Absorption chiller

A steam extraction upstream of the LP turbine was set to drive absorption chillers. In order to fix the extraction pressure level, it was necessary to control LP turbine by means of a throttle valve, downstream of the steam extraction point. So saturated steam is delivered to the chillers at constant pressure (7.7 bar), whatever the flow rate through the LP turbine. When the cooling demand is high, the valve upstream of the LP turbine is closed so that the highest available steam flow rate is sent to the chillers. Condensate flow exiting the chillers at 3.15 bar and 99°C is returned to the condenser hot well. Four Li-Br two-stage absorption chiller units, for a total cooling capacity of 82.8 MW, have been supposed to be installed. Each units has a nominal capacity of 20.7 MW and COP of 1.31.

2.4. Reference combined cycle

The conventional fossil fuel combined cycle considered as a reference was sized to match the peak power demand in the summer day since compression chillers alone are assumed to provide the required cooling load. Accordingly the SGT-1000F, rated 67.4 MWe, was selected among Siemens gas turbines. Design criteria for the steam cycle block were the same as those applied to the ISCC. The resulting CC design performance at ISO conditions are reported in Table 3. GT off-design operation was considered depending on ambient temperature and humidity, as previously explained in section 2.2. SGT -800 and SGT-1000F have similar load control. However, in the latter, IGV can be modulated up to 50% full load (Fig. 8).

3. Simulation method and assumptions

Trnsys® with the model libraries STEC (developed by DLR) and TESS was used to model PTC solar field and absorption chillers operation, whereas the power blocks were modeled by Thermoflex®. This allowed for taking the best of both codes to achieve accurate off design simulations. In fact, Trnsys® is a flexible, graphically based software environment used to simulate the behavior of transient systems, with a focus on assessing the performance of thermal

216 systems including renewable energy and solar components. Thermoflex® is a modular program with a graphical
 217 interface that allows the user to assemble a model from icons representing plant components. The program models all
 218 types of power plants, with a strong emphasis on combined cycle and conventional steam plants, and covers both design
 219 and off-design simulation, in a steady environment. Specifically, a design procedure was carried out in order to define
 220 mass and heat balances of each cycle component. Once proper sizing and stand-alone performance of every component
 221 have been achieved, the cycle model was assembled and operated in off-design conditions. An extensive library of
 222 components, including real GT models, facilitates designing plants based on typical practice of today.

223 The Trnsys® model of the solar field provides exit heat transfer fluid (HTF) flow rate and temperature based on climate
 224 conditions. These values are transferred to Thermoflex® as an input for the HTF source. Geometrical details of PTC are
 225 summarized in Table 4. The overall efficiency of a parabolic trough collector is a function of both the fraction of direct
 226 normal radiation absorbed by the receiver (optical efficiency) and the heat lost to the environment when the receiver is
 227 at operating temperature. The PTC overall efficiency η_{PTC} under actual operating conditions was evaluated as follow:

$$228 \quad \eta_{PTC} = K[A + B(\Delta T)] + C \frac{\Delta T}{I_b} + D \frac{\Delta T^2}{I_b} \quad (1)$$

229 The η_{PTC} formula was derived from [18]. The incident angle modifier K takes into account the effect of the non-
 230 perpendicularity of solar radiation and it is a function of the incidence angle Ia :

$$231 \quad K = \cos(Ia) - 0.0003512(Ia) - 0.00003137(Ia)^2 \quad (2)$$

232 In Eq. (1) A accounts for the optical efficiency of the trough and the absorptivity of the absorber tube selective coating;
 233 B , C and D describe the heat losses of the heat collector element with ΔT as the temperature difference between the
 234 HTF and the ambient. I_b is the actual beam radiation. Values of coefficients A (0.77), B (-0.022), C (0.5) and D (-0.033)
 235 were computed to fit the thermal efficiency curve of Schott PTR70 receivers under standard conditions [19].

236 The absorption chillers were modeled according with performance maps taken from manufacturer's catalogs. Fig. 9
 237 shows the normalized performance data related to the part-load operation of the chiller. This approach allows to
 238 accurately predict the off-design behavior of the absorption unit, depending on the steam mass flow rate supplied by the
 239 combined cycle. As far as the mechanical compression chillers is concerned, COP was assumed to decrease linearly
 240 with increasing ambient temperature. The resulting COP is slightly higher than 4 at outdoor temperature of 15°C; it
 241 goes down to 2.2 in hot weather, at 40°C.

242 The location selected for the present analysis was assumed to have climatic conditions and latitude corresponding to
 243 those of Abu Dhabi (UAE). Meteonorm database from the Trnsys® weather library provided the meteorological data
 244 for the daily simulations. Meteorological conditions in terms of ambient temperature (Fig. 10) and direct normal
 245 irradiation profiles (Fig. 11) are reported for the two selected days, chosen as representative of a typical summer and

246 winter day.

247 The modeling of the SCCP plant was carried out according to the following logic:

248 1. during the day the solar source has the highest priority, so the whole available solar steam flow rate contributes to the
249 power generation;

250 2. the steam flow rate sent to the absorption chillers is computed to follow the cooling demand. When the highest
251 available steam flow rate at the extraction point is not enough to cover the cooling need, compression chillers are
252 assumed fill the gap between the required and the available cooling load, thus increasing the electric power demand;

253 3. the GT load is computed to match the new value of the power load.

254 Steps 2 to 3 are repeated until both cooling and power load are matched as they vary daily.

255

256 **4. Results and discussion**

257 A compendium of the simulation results is here presented. Performance data of the SCCP plant are compared, under
258 same load and cooling demand profile, to those of the reference CC. It has to be underlined that in order to meet the
259 island operation mode of the system, the plant management logic was assumed to always cover peak electricity demand.
260 Under these operating conditions the absorption chillers did not allow to cover the whole cooling demand during the
261 summer day, as shown in Fig. 12. This is because the low pressure steam flow rate available for the chillers is not
262 enough to ensure the huge amount of cooling load from early in the morning up to late in the evening. Thus
263 compression chillers are used to fill the gap with respect to the overall cooling load. During the winter day (Fig. 13), the
264 request of cooling is reduced by a factor of about 5. Consequently only a small part of the available steam flow rate is
265 extracted to drive the absorption chillers; all the remaining steam is sent to the LP turbine section for power production.
266 The cooling load demand is completely satisfied by absorption chillers, meaning that in the winter day there is no need
267 for compression chillers.

268 Figs. 14-15 show hour by hour power production of the SCCP in summer and winter days, while results for the
269 reference CC plant are presented for comparison in Figs. 16 -17. For the SCCP plant the introduction of the absorption
270 chillers makes the original grid load levels (green, solid line) to be lowered down to the “residual electric demand”. The
271 difference between the total and the residual electric demand quantifies the daily electric energy saving deriving from
272 the usage of absorption chillers instead of compression chillers. As a result, the peak power in the summer day
273 (corresponding also to the annual peak) decreases of about 25 MW. This means that the rated power of both combined
274 cycle and gas turbine to be installed in the system can be consistently reduced, with a significant decrease in the
275 investment costs.

276 Looking at the data of Figs. 14 and 15 the contribution coming from the CSP section during sunny hours is evident. In

fact the gas turbine is called to provide an almost constant power output (GT P_{el}) both in day and night hours. This because, despite the steam flow delivered to the absorption chillers, the solar contribution to the steam production makes the steam turbine able to produce roughly about 20 MW (ST P_{el}) in the peak hours, both in winter and summer. The GT load is determined so to match hour-by-hour the residual power demand. The GT power output depends on the ambient temperature and also on the solar steam production. It can be observed that the GT load goes down when the ST P_{el} increases due to the solar contribution. Accordingly, in the daylight hours of the winter day (Fig. 15) the resulting ST P_{el} is even higher than the GT P_{el} . Conversely, during the night hours of the summer day (Fig. 14), the GT has to cover roughly the whole power demand since most of the LP steam is used to drive absorption chillers instead of flowing through the LP turbine.

For the reference CC plant the load-following strategy is much easier than for SCCP (Figs. 16 - 17), as it has been sized to match the total electric demand. In this case the total and the residual electric demand coincide. The GT load is the only variable that can be changed to ensure that the sum of ST P_{el} and GT P_{el} is equal to the electricity request. In the peak hour of the summer day, the GT generates about 56 MW_{el} (67% of the total load) while in the peak hour of the winter day the GT power output goes down to about 25 MW_{el}, i.e. 59% of the total load.

In order to better describe the plant operation, the GT load profiles in the SCCP and the CC plants were compared against each other in Fig. 18. The GT load is evaluated as a percentage of the design rated power. As expected, the GT in the CC plant runs at full load only in the peak hour of the summer day, coherently with the CC plant sizing assumptions. In summer, the GT load in the SCCP plant is always greater than 50% and over 90% for the afternoon hours up to 9 pm. It is important to note that during the night hours of both winter and summer day, the SCCP system allows to operate the GT at higher load than in the CC plant, thus resulting in higher GT efficiency. The reader is reminded that the SGT-800 rating is about 70% of the SGT-1000F. Coherently, the CC plant was found to undergo much wider variations in the GT load to ensure the required electric and cooling load all over the day. Fig. 19 clearly demonstrates the penalty in the GT efficiency η_{GT} which affects the performance of the CC plant during the night hours of both the investigated days, with respect to the SCCP system. η_{GT} represents the gas turbine efficiency computed from the following:

$$\eta_{GT} = \frac{GT P_{el}}{m_{fuel} * LHV} * 100 \quad (3)$$

This penalty is more relevant in winter when the GT works at extreme off design conditions.

To demonstrate the benefits of the SCCP system with respect to the CC solution, the fossil fuel consumption have been computed for both days (Fig. 20). The SCCP plant requires much lower fuel flow all over the 24 hours, both in summer and winter day, as compared to CC. In particular, the SCCP system is shown to reduce the fossil fuel consumption by

about 40% for both summer peak hour (2.1 kg/s against 3.6 kg/s) and winter one (1.3 kg/s against 2.1 kg/s). This, of course, is the combined result of the solar energy contribution and the adoption of absorption chillers. A significant amount of fossil fuel is saved also during night hours. This is due not only to absorption chillers, but also to higher load and efficiency of the SGT-800, compared to the SGT-1000F.

To better compare the SCCP system performance against the CC, the following plant efficiency was defined:

$$\eta = \frac{Pel_{CC} + Pth_{ABS} COP_{ABS} / COP_{Comp}}{m_{fuel} LHV} * 100 \quad (4)$$

In (3) the power produced by the combined cycle (CC P_{el}) is added to the electricity savings deriving from the use of absorption chillers (ABS) instead of compression chillers (Comp). Pth_{ABS} accounts for the thermal input of the absorption chillers; m_{fuel} corresponds to the fossil fuel consumption shown in Fig. 20. It is reminded that COP_{ABS} equals 1.31 and COP_{Comp} varies with outdoor temperature in the range between 2.2 and 4. The resulting values of the overall efficiency η are shown in Fig. 21. The SCCP plant was found to be more efficient than the CC through the whole day, both in summer and winter. The solar steam contribution to the SCCP efficiency can be clearly identified during the daylight hours: η increases up to about 70% and 85% in winter and summer, respectively.

Performance data have been integrated over all the 24 hours of both days and the relevant results are summarized in Tables 5 and 6. In both days, the SCCP can meet cooling and power demand with an electricity production significantly lower than the CC one. This is the effect of using absorption chillers instead of compression chillers for cooling generation. Actually the SCCP is required to cover only a fraction of the load profile, i.e. the one defined as “residual electric demand”. Moreover the efficiency of SCCP defined as in (4) is much higher. The average overall efficiency for SCCP in the summer day is 68.5% vs. 46.1%. It has to be underlined that this so high value is mostly due to the solar contribution. In the winter day an efficiency gain of about 5% is also achieved (42.3% vs. 37.4%). But the most relevant point is the fossil fuel saving. The SCCP is much better than CC as the fuel consumption in summer is reduced by 33%, i.e. from 3210 MWh down to 2152 MWh, while in winter by 26%, i.e. from 2063 MWh, down to 1528 MWh. It is also interesting to point out that the solar energy contributes to fuel savings by 43% of the total in summer, while the use of absorption chillers is contributing by 57%. In winter the contribution of solar energy to fuel saving is lower, but in percentage it increases up to 70%. Finally, no relevant contribution was found to come from the higher load factor of GT units.

5. Conclusions

In this work a SCCP plant including a combined cycle gas turbine SGT-800, a PTC solar field and double-effect steam driven absorption chillers, was modeled in details. Plant performance was compared against that of a conventional pure-

339 fossil solution based on a combined cycle gas turbine SGT-1000F and compression chillers. Both the systems matched
340 the same load and cooling demand. In addition, they were designed to operate in “island mode” according with a load-
341 following logic. Simulations were carried out for climate and latitude corresponding to Abu Dhabi to resemble a remote
342 area in hot climate.

343 The use of absorption chillers fed by low grade steam allows to reduce the actual electric power requested to the SCCP
344 system. Accordingly, the rated power of both combined cycle and gas turbine to be installed in the SCCP plant is lower
345 than that in the pure fossil CC system, with significant reduction of investment costs. Moreover, the integration of the
346 solar steam helps to mitigate peak demand charges, especially in the summer day.

347 To summarize, the SCCP plant shows the following advantages over the conventional pure-fossil CC: i) smaller GT
348 power: SGT-800 instead of SGT-1000F; ii) higher overall efficiency both in summer and winter days; iii) significant
349 fossil fuel savings in summer (-33%) and winter (-26%). The contribution to such a significant fuel saving comes from
350 the solar power integration in the system and the use of absorption chillers, with a different weight depending on
351 ambient conditions.

352

353

354 **References**

- 355 [1] O. Erdinc, M. Uzunoglu, Optimum design of hybrid renewable energy systems: Overview of different approaches,
356 Renewable and Sustainable Energy Reviews 16 (2012) 1412–1425.
- 357 [2] N. Hatziaargyriou, G. Contaxis, M. Matos, J.A.P. Lopes et al., Energy management and control of island power
358 systems with increased penetration from renewable sources, in Proc. of IEEE Power Engineering Society Winter
359 Meeting 1 (2002) 335-339.
- 360 [3] V. Cosentino, S. Favuzza, G. Graditi, M. G. Ippolito et al., Smart renewable generation for an islanded system.
361 Technical and economic issues of future scenarios, Energy 39 (2012) 196–204.
- 362 [4] R. R. Obaid, Reducing peak electricity demand trough 300MW wind farm North of Jeddah, Saudi Arabia,
363 International Journal of Engineering & Technology 11 (2011) 151-157.
- 364 [5] A. M. Al-Ibrahim, A. Varnham, A review of inlet air-cooling technologies for enhancing the performance of
365 combustion turbines in Saudi Arabia, Applied Thermal Engineering 30 (2010) 1879–1888.
- 366 [6] M. Ameri, S. H. Heiazi, K. Montaser, Performance and economic of the thermal energy storage systems to enhance
367 the peaking capacity of the gas turbines, Applied Thermal Engineering 25 (2005) 241-251.
- 368 [7] M. Ameri, S.H. Hejazi, The study of capacity enhancement of the Chabahar gas turbine installation using an
369 absorption chiller, Applied Thermal Engineering 24 (2004) 59–68.
- 370 [8] K.K. Yum, G. Grozev, M. James, J. Page, Solar Power Supply to Mitigate the Diurnal and Seasonal Electricity
371 Demand in Victoria, in Proc. of Solar2010, the 48th AuSES Annual Conference, 1-3 December 2010, Canberra,
372 Australia.
- 373 [9] F.J. Cabrera, A. Fernández-García, R.M.P. Silva, M. Pérez-García, Use of parabolic trough solar collectors for solar
374 refrigeration and air-conditioning applications, Renewable and Sustainable Energy Reviews 20 (2013) 103-118.
- 375 [10] Ahmed Y. Taha Al-Zubaydi, Solar Air Conditioning and Refrigeration with Absorption Chillers Technology in
376 Australia – An Overview on Researches and Applications, Journal of Advanced Science and Engineering Research 1
377 (2011) 23-41.
- 378 [11] F. Calise, High temperature solar heating and cooling systems for different Mediterranean climates: Dynamic
379 simulation and economic assessment, Applied Thermal Engineering 32 (2012) 108-124.
- 380 [12] P. Palenzuela, G. Zaragoza, Diego C. Alarcón-Padilla, J. Blanco, Evaluation of cooling technologies of
381 concentrated solar power plants and their combination with desalination in the mediterranean area, Applied Thermal
382 Engineering 50 (2013) 1514–1521.
- 383 [13] N. Phuangpornpitaka, S. Tia, Opportunities and challenges of integrating renewable energy in smart grid system,
384 Energy Procedia 34 (2013) 282-290.

385 [14] J. Wang, A. J. Conejo, C. Wang, J. Yan, Smart grids, renewable energy integration, and climate change mitigation
386 – Future electric energy systems, *Applied Energy* 96 (2012) 1-3.

387 [15] M.A. Abdullah, A.P. Agalgaonkar, K.M. Muttaqi, Assessment of energy supply and continuity of service in
388 distribution network with renewable distributed generation, *Applied Energy* 113 (2014) 1015–1026.

389 [16] M. Marwan, F. Kamel, Smart grid demand side response model to mitigate peak demands on electrical networks,
390 *Journal of Electronic Science and Technology* 9 (2011) 136-144.

391 [17] N. Li, L. Chen, S. H. Low, Optimal Demand Response based on utility maximization in power networks, in *Proc.*
392 *of IEEE Power Engineering Society General Meeting* (2011) 1-8.

393 [18] F. Lippke, Simulation of the Part-Load Behavior of a 30 MWe SEGS Plant, Sandia National Labs. Report SAND--
394 95-1293, 1995.

395 [19] T. Moss, D. Brosseau, D., Testing capabilities NSTTF (AZTRAK) rotating platform. Sandia National laboratories,
396 New Mexico, 2007.

397 [20] C.D Moné, D.S Chau, P.E Phelan, Economic feasibility of combined heat and power and absorption refrigeration
398 with commercially available gas turbines, *Energy Conversion and Management* 42 (2001), 1559–1573.

399 [21] S. Popli, P. Rodgers, V. Eveloy, Trigeneration scheme for energy efficiency enhancement in a natural gas
400 processing plant through turbine exhaust gas waste heat utilization, *Applied Energy* 93 (2012), 624–636.

401 [22] A. Khaliq, Exergy analysis of gas turbine trigeneration system for combined production of power heat and
402 refrigeration, *International Journal of Refrigeration* 32 (2009), 534–545.

403

404

405

406

407

408

409 **Figure captions**

- 410 **Fig. 1.** Power load and cooling profiles in the summer day.
- 411 **Fig. 2.** Power load and cooling profiles in the winter day.
- 412 **Fig. 3.** Schematic of the investigated SCCP plant.
- 413 **Fig. 4.** Schematic of the investigated SCCP plant: screenshot of Thermoflex®.
- 414 **Fig. 5.** HTF/steam HX T-Q diagram.
- 415 **Fig. 6.** GT power generation: manufacturer's data vs. simulation output.
- 416 **Fig. 7.** Effects of load control on SGT-800 firing and exhaust temperature.
- 417 **Fig. 8.** Effects of load control on SGT-1000F firing and exhaust temperature.
- 418 **Fig. 9.** Two-stage absorption chiller performance map.
- 419 **Fig. 10.** Patterns of daily ambient temperature.
- 420 **Fig. 11.** Patterns of daily solar irradiation.
- 421 **Fig. 12.** Cooling load curve in the summer day.
- 422 **Fig. 13.** Cooling load curve in the winter day.
- 423 **Fig. 14.** SCCP plant electricity production in the summer day.
- 424 **Fig. 15.** SCCP plant electricity production in the winter day.
- 425 **Fig. 16.** CC plant electricity production in the summer day.
- 426 **Fig. 17.** CC plant electricity production in the winter day.
- 427 **Fig. 18.** SCCP vs. CC: Gas Turbine load.
- 428 **Fig. 19.** SCCP vs. CC: Gas Turbine efficiency.
- 429 **Fig. 20.** SCCP vs. CC: Fossil fuel consumption.
- 430 **Fig. 21.** SCCP vs. CC: Overall Efficiency.

431 **Table 1**

432 Design parameters of the CC in fossil fuel operation (ISO condition).

Design Parameter	Value
GT Power Output (MW _e)	46.4
GT Efficiency (%)	37.0
GT Pressure ratio	19.9
GT exhaust gas flow (kg/s)	131.5
GT exhaust gas T (°C)	548
HP - LP pressures (bar)	69-7.7
HP - LP SH temperatures (°C)	522– 218
HP - LP steam flow (kg/s)	16.4 - 19.8
Condenser pressure (bar)	0.06
ST Power (MW _e)	20.8
CC net Power Output (MW _e)	66.5
Fuel Consumption (MW _{th})	124.4
CC net efficiency (%)	53.5

433

434 **Table 2**

435 Design parameters of the ISCC with the highest solar contribution.

Design Parameter	Value
Maximum solar steam flow rate (kg/s)	32.3
Solar HX thermal power (MW _{th})	75.6
Net power output (MW _e)	94.3

436

437 **Table 3**

438 Design parameters of the reference CC (ISO condition).

Design Parameter	Value
GT Power Output (MW _e)	67.4
GT Efficiency (%)	35.3
Pressure ratio	15.8
GT exhaust gas flow (kg/s)	190.3
GT exhaust gas T (°C)	583
HP - LP pressures (bar)	69-7.7
HP - LP SH temperatures (°C)	522– 218
HP - LP steam flow (kg/s)	28.4 – 32.3
Condenser pressure (bar)	0.06
ST Power (MW _e)	35.0
CC net Power Output (MW _e)	99.3
Fuel Consumption (MW _{th})	189.7
CC net efficiency (%)	52.4

439

440 **Table 4**

441 Geometrical and optical parameters of PTC.

Design Parameter	Value
Alignment	North-South
Total collector area (m ²)	150,000
Length of single collector assembly (m)	47
Aperture width of single collector assembly (m)	5.6
Focal length of single collector assembly (m)	1.668

442
443

444 **Table 5**

445 SCCP vs. CC: Performance in the summer day.

	SCCP	CC
Electricity production (MWh)	919.7	1,497.9
Average GT load (%)	73.3	66.9
Average overall efficiency η (%)	68.5	46.1
Fossil Fuel Input (MWh)	2152.3	3210.3
Fossil fuel saving (MWh):	1058.0 (-33%)	--
- due to solar input	455 (43%)	
- due to absorption chiller	603 (57%)	

446

447 **Table 6**

448 SCCP vs. CC: Performance in the winter day.

	SCCP	CC
Electricity production (MWh)	646.0	779.9
Average GT load (%)	34.7	27.9
Average overall efficiency η (%)	42.3	37.4
Fossil Fuel Input (MWh)	1528.9	2063.3
Fossil fuel saving (MWh):	534.4 (-26%)	
- due to solar input	374 (70%)	
- due to absorption chiller	160.4 (30%)	

449

Figure1
[Click here to download high resolution image](#)

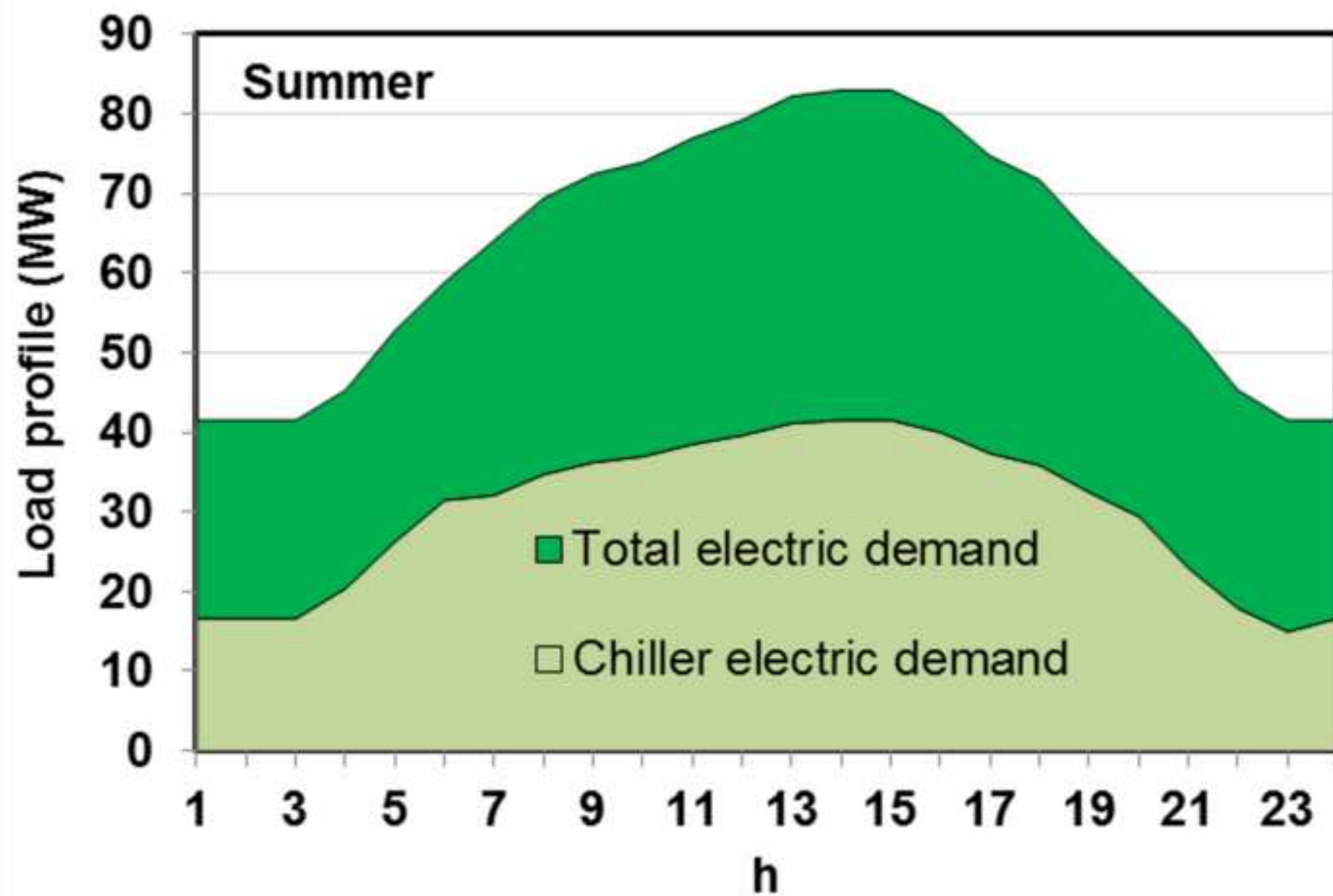


Figure2

[Click here to download high resolution image](#)

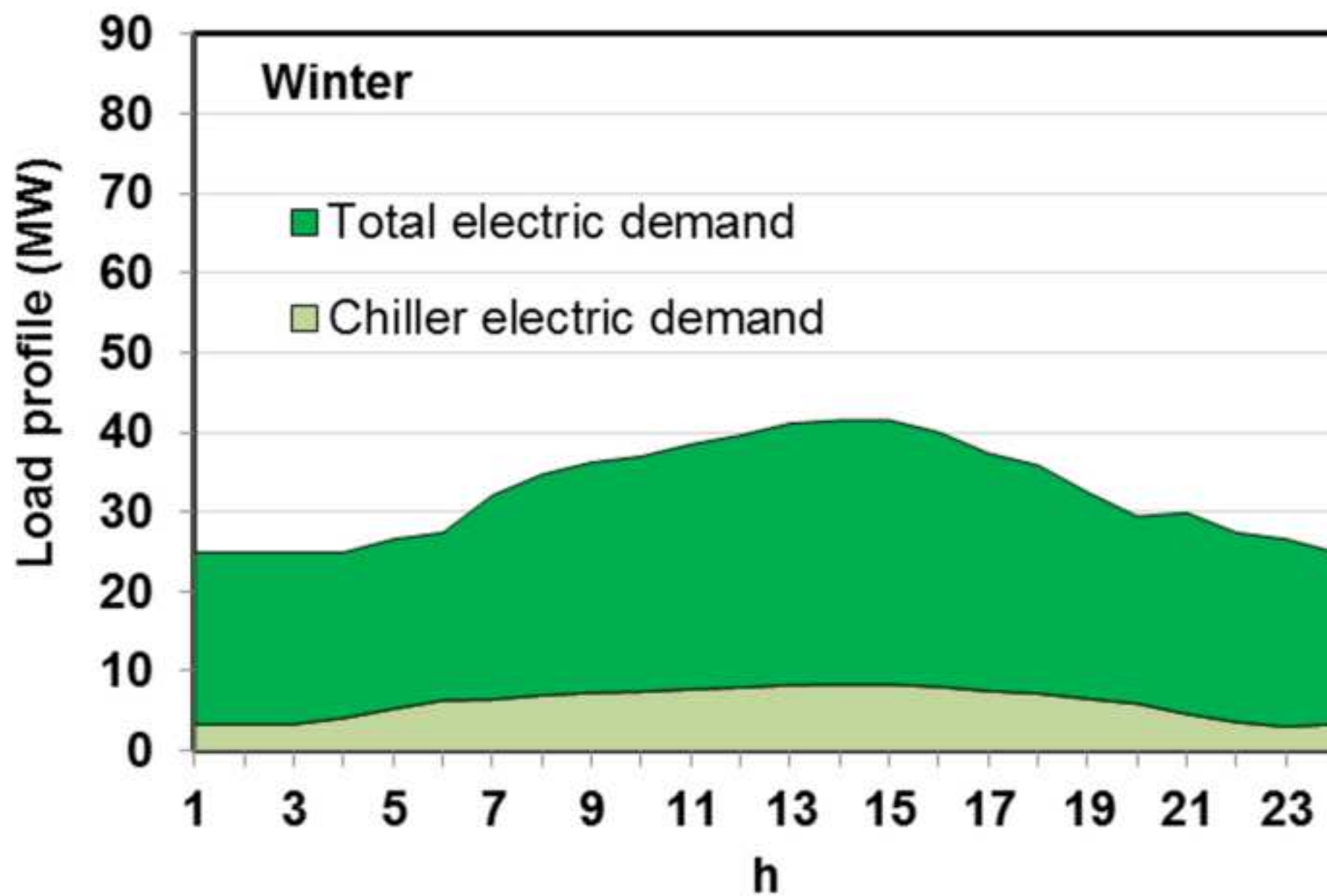


Figure3

[Click here to download high resolution image](#)

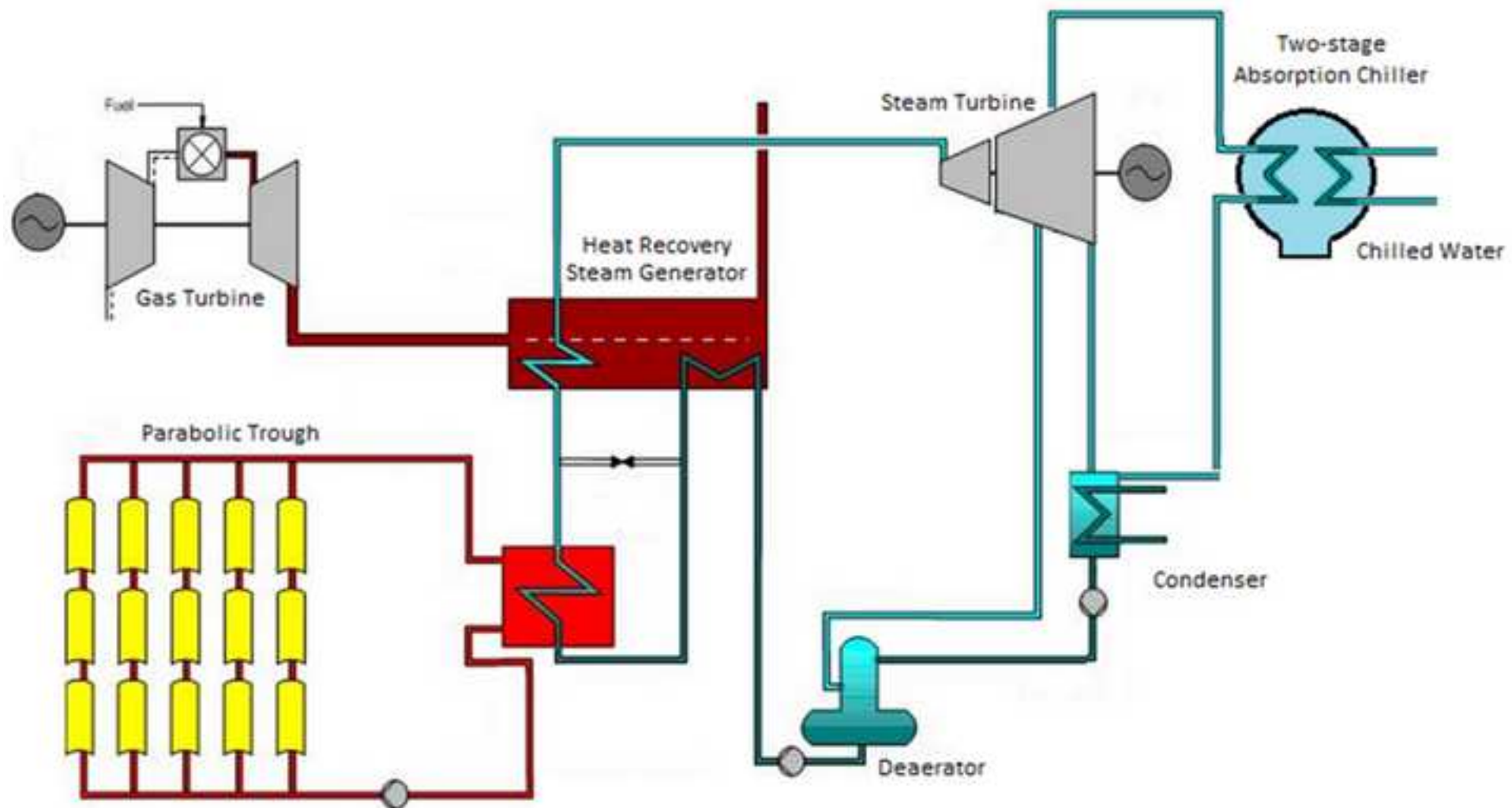


Figure4

[Click here to download high resolution image](#)

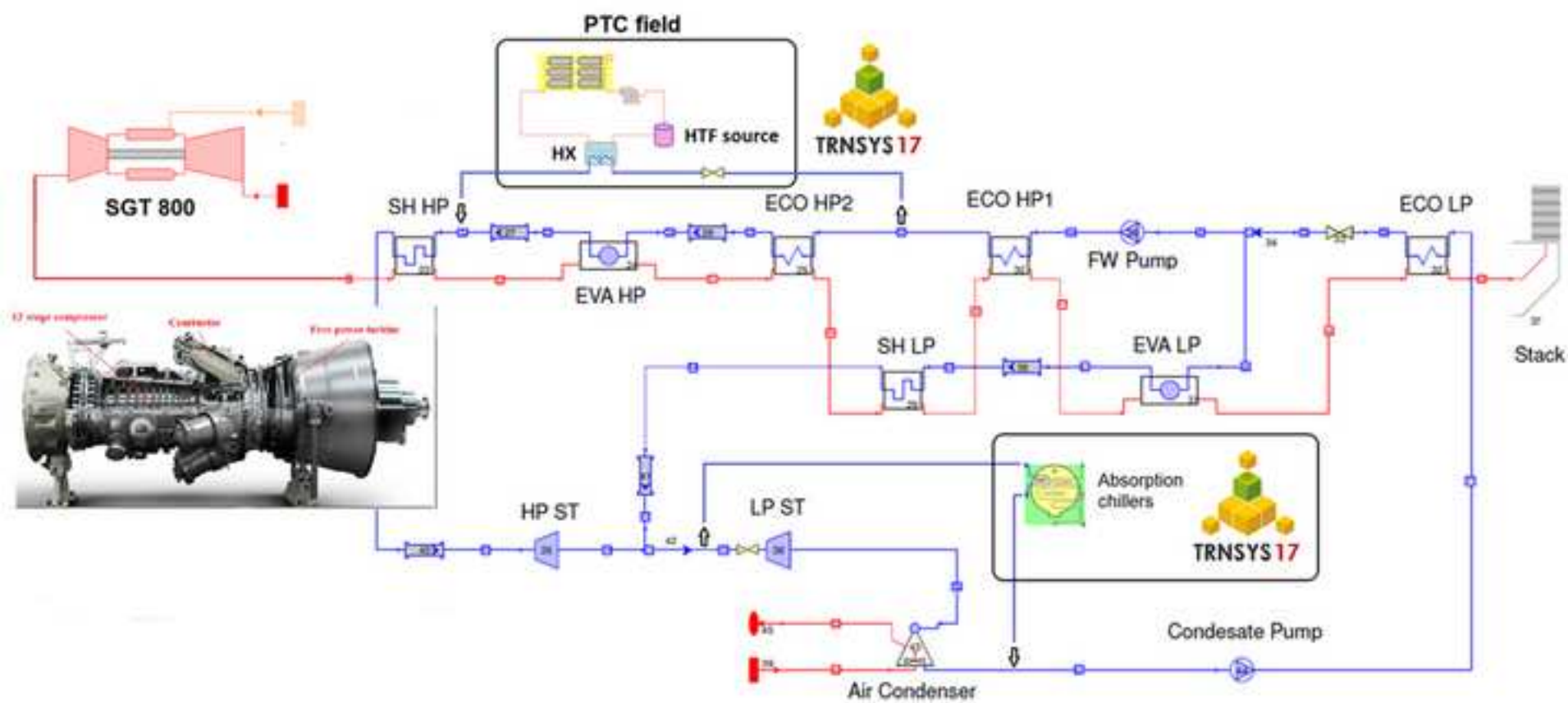


Figure5

[Click here to download high resolution image](#)

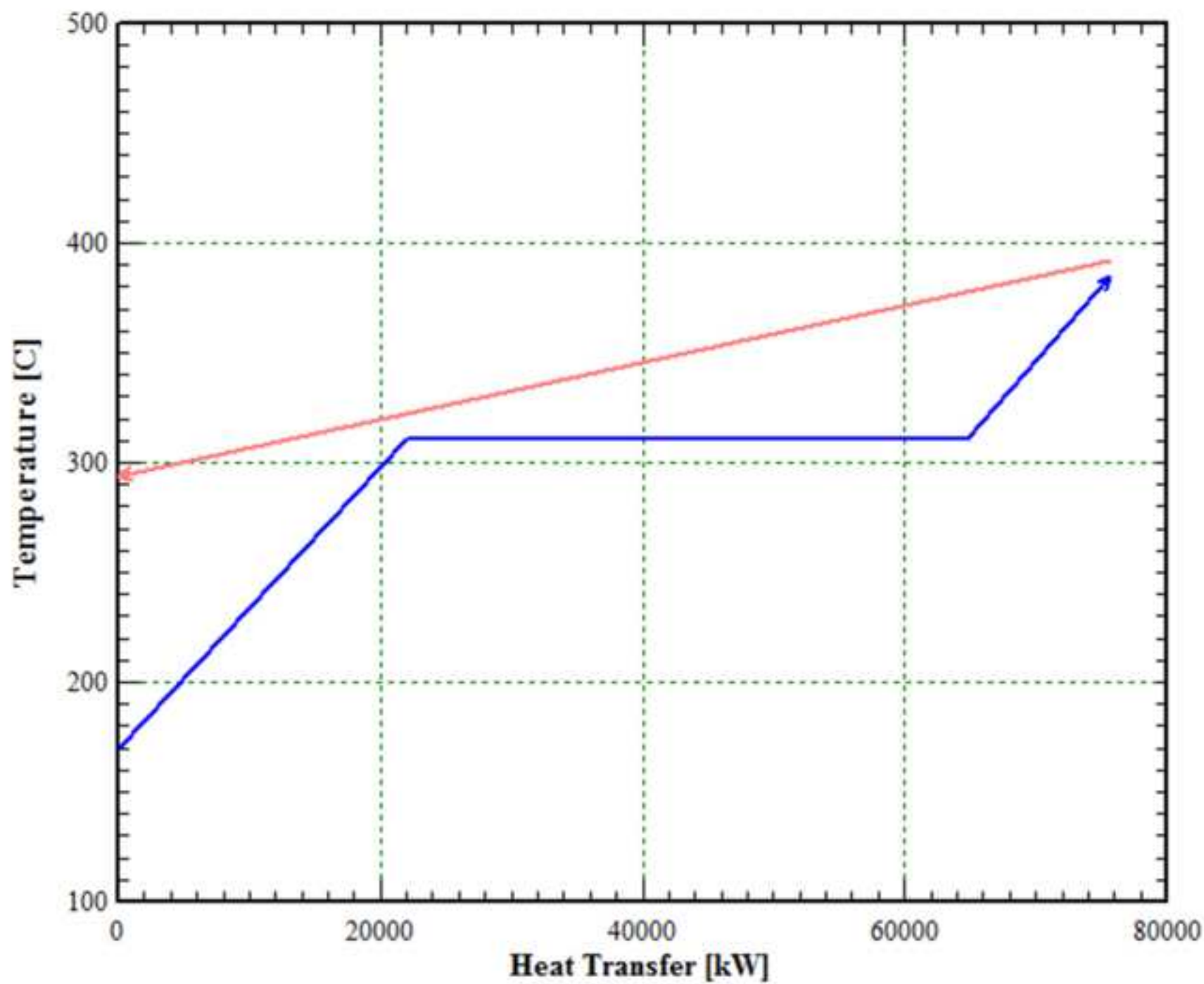


Figure6

[Click here to download high resolution image](#)

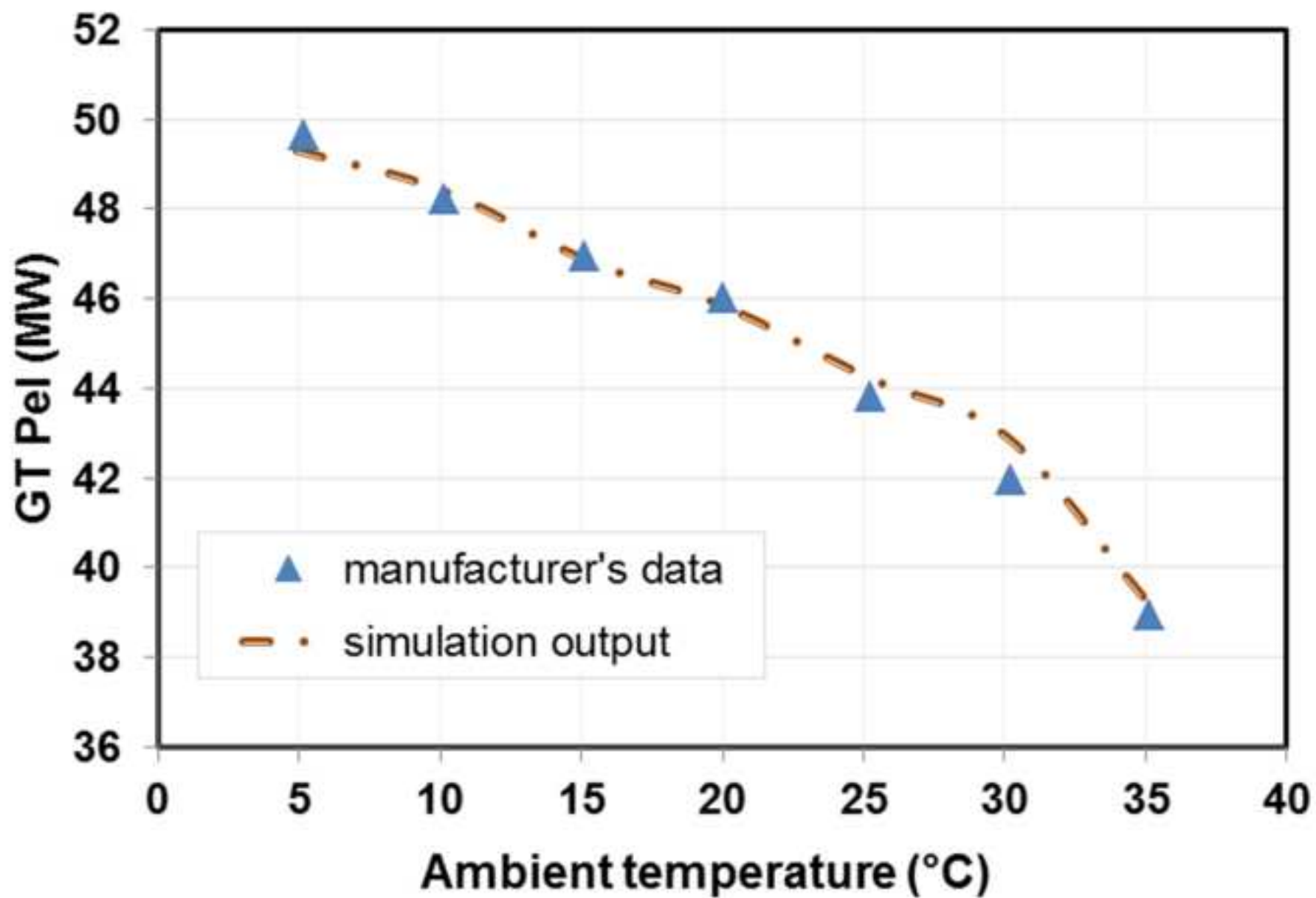


Figure7

[Click here to download high resolution image](#)

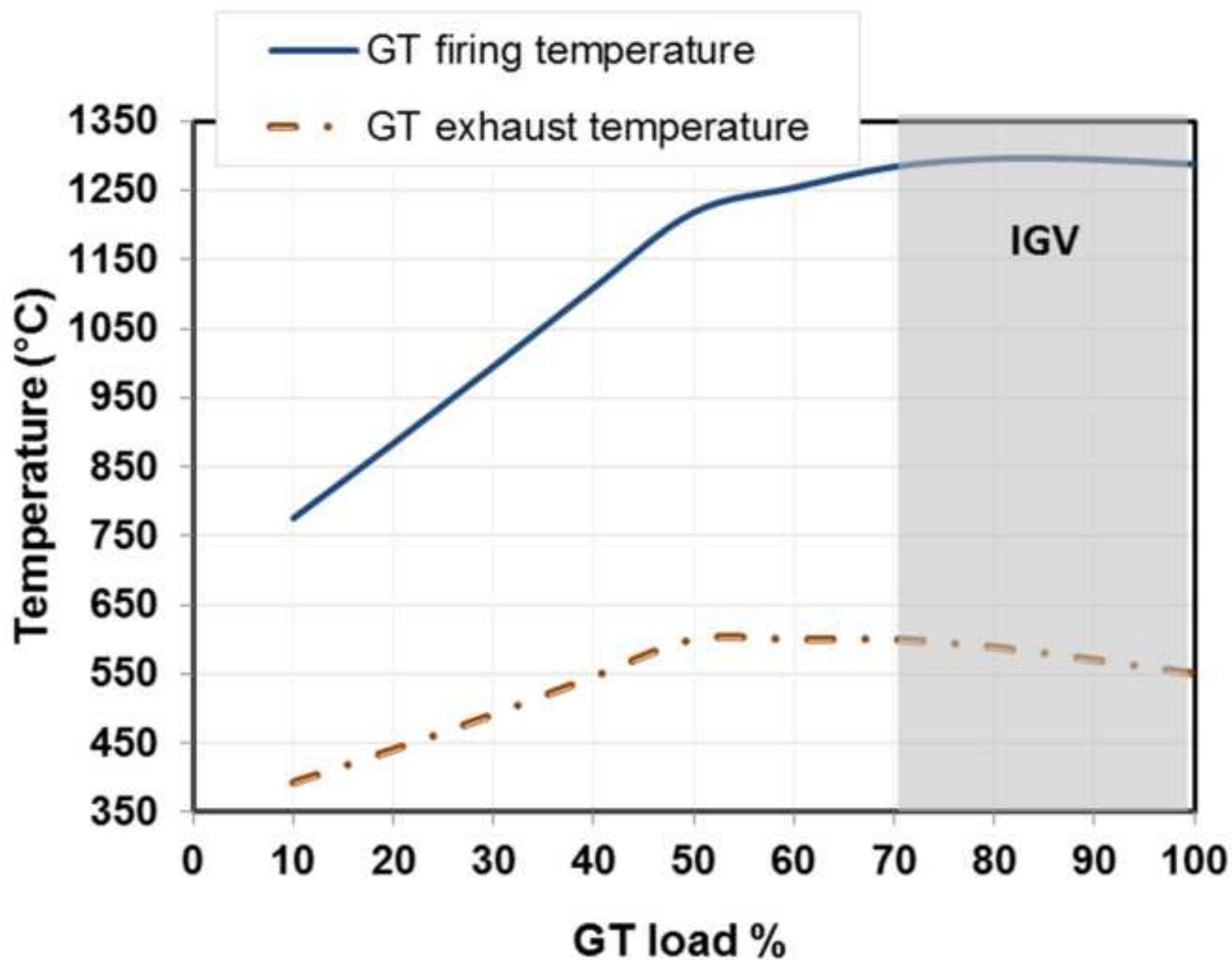


Figure8

[Click here to download high resolution image](#)

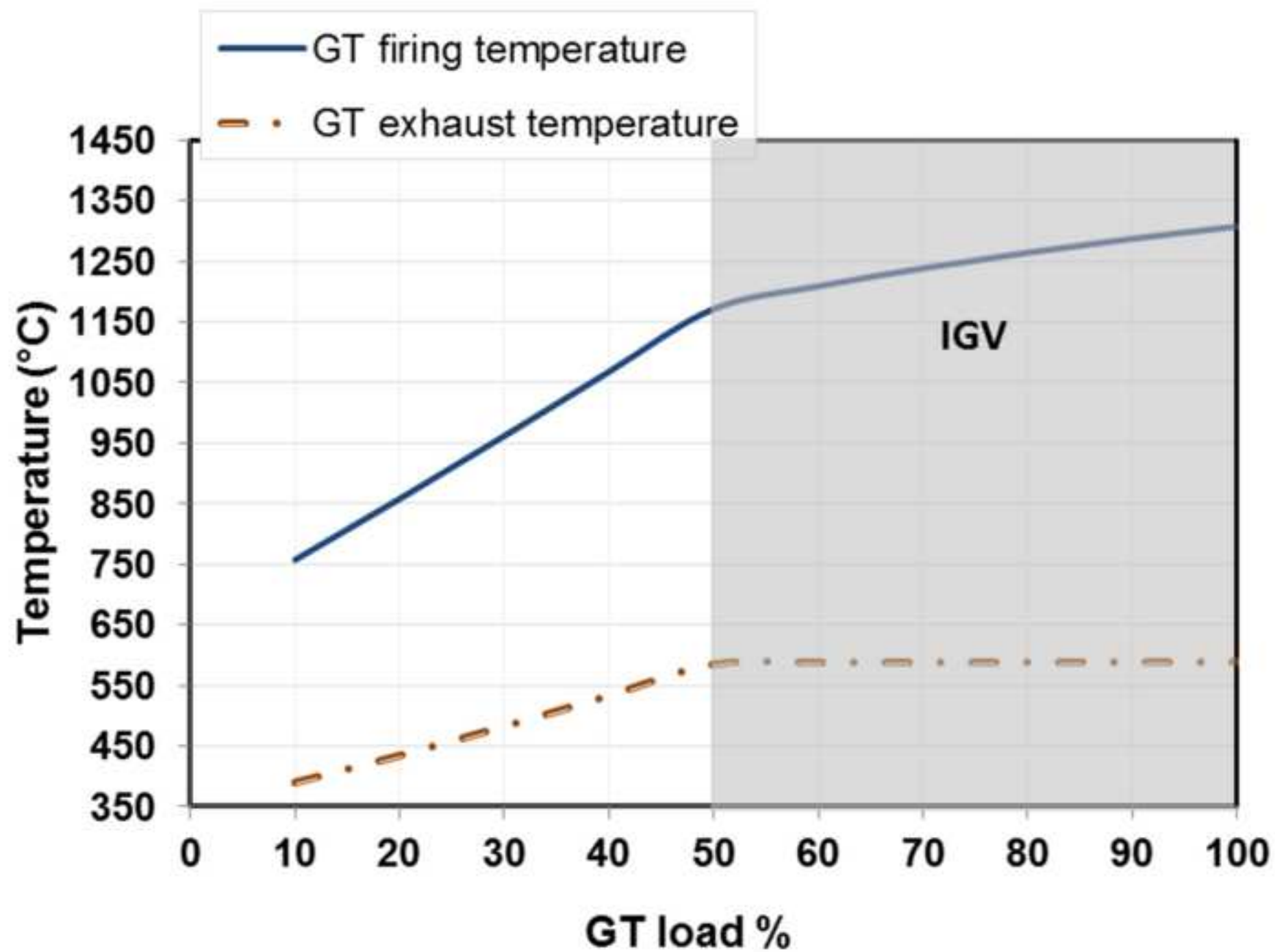


Figure9

[Click here to download high resolution image](#)

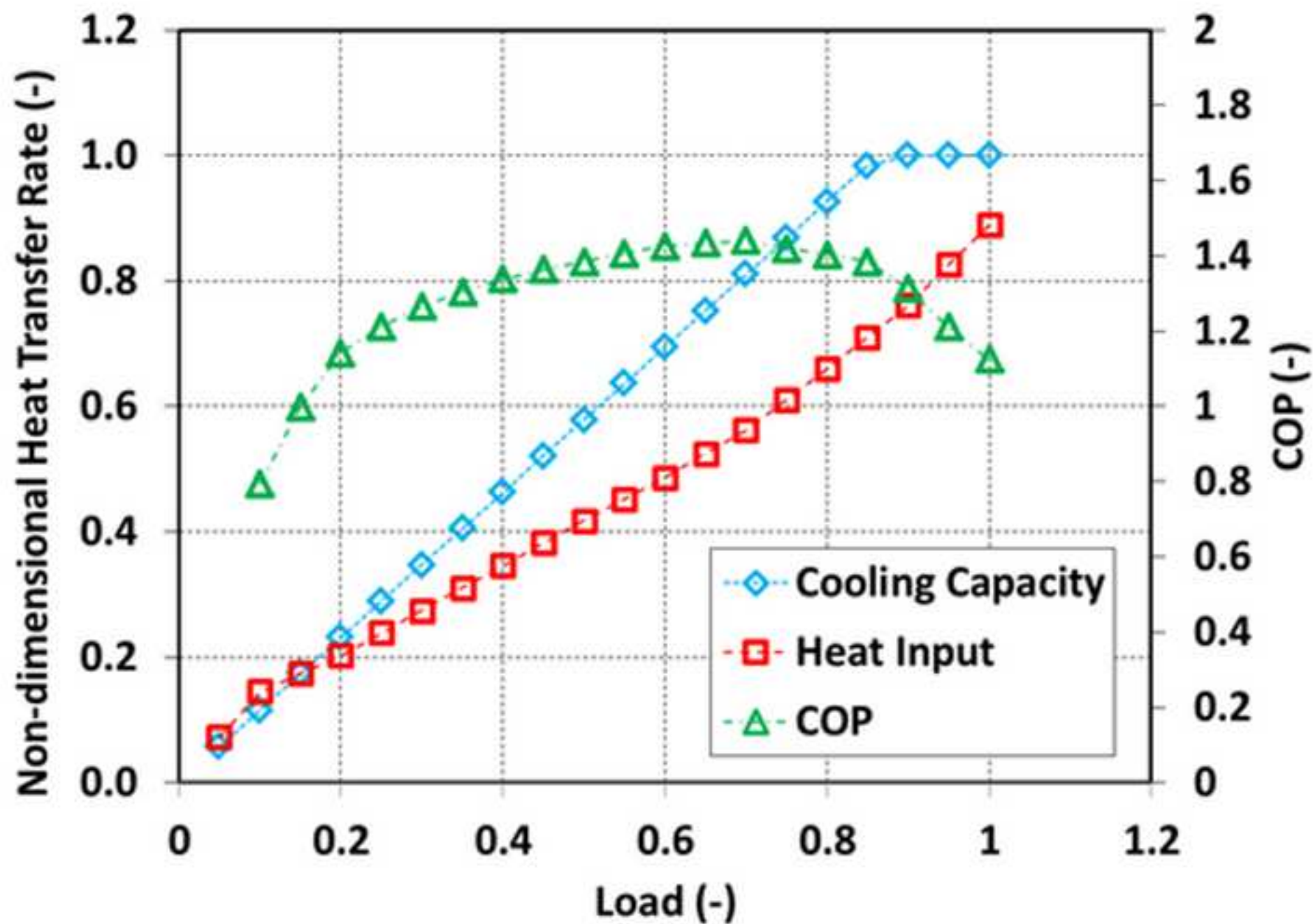


Figure10
[Click here to download high resolution image](#)

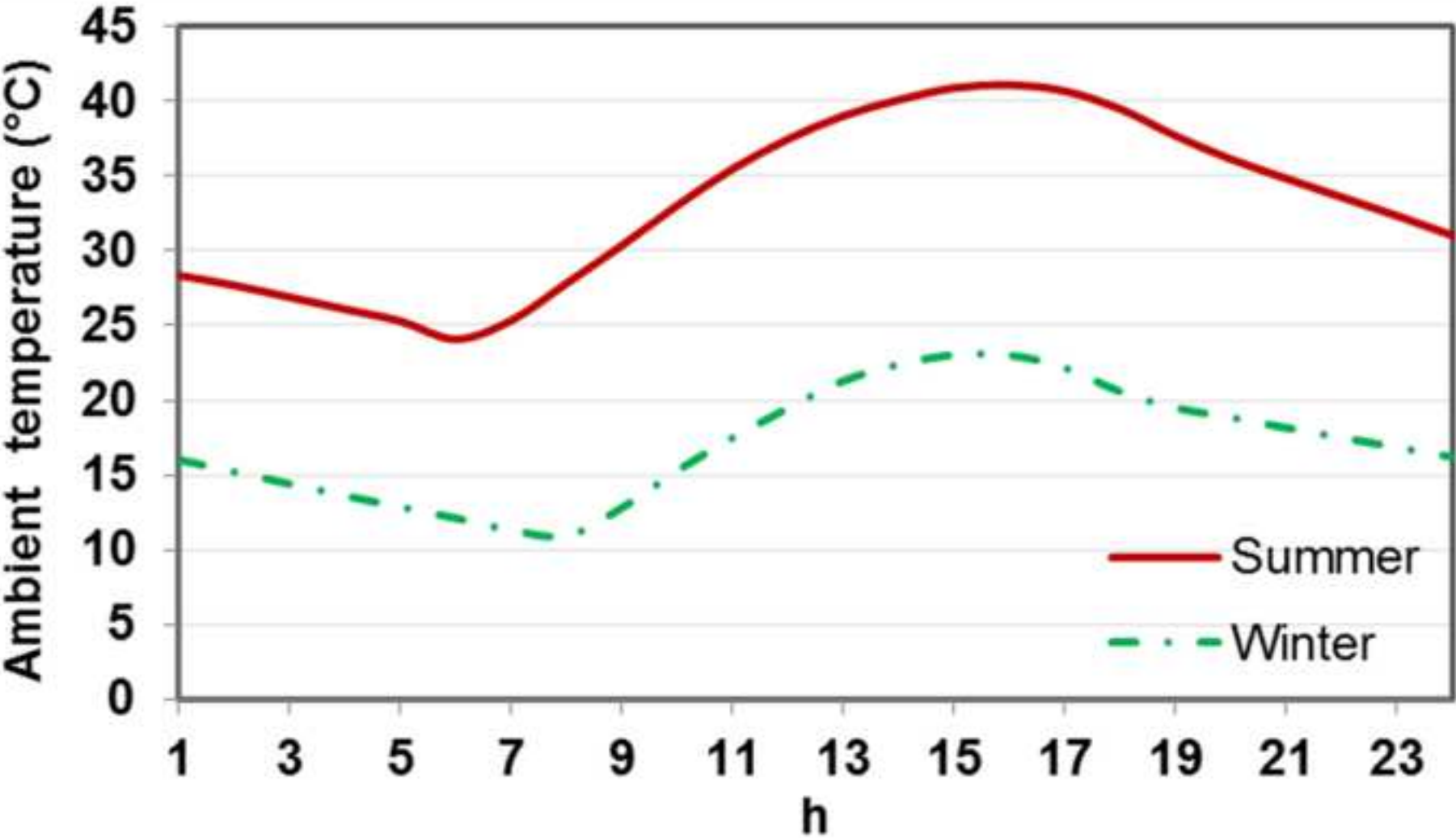


Figure11
[Click here to download high resolution image](#)

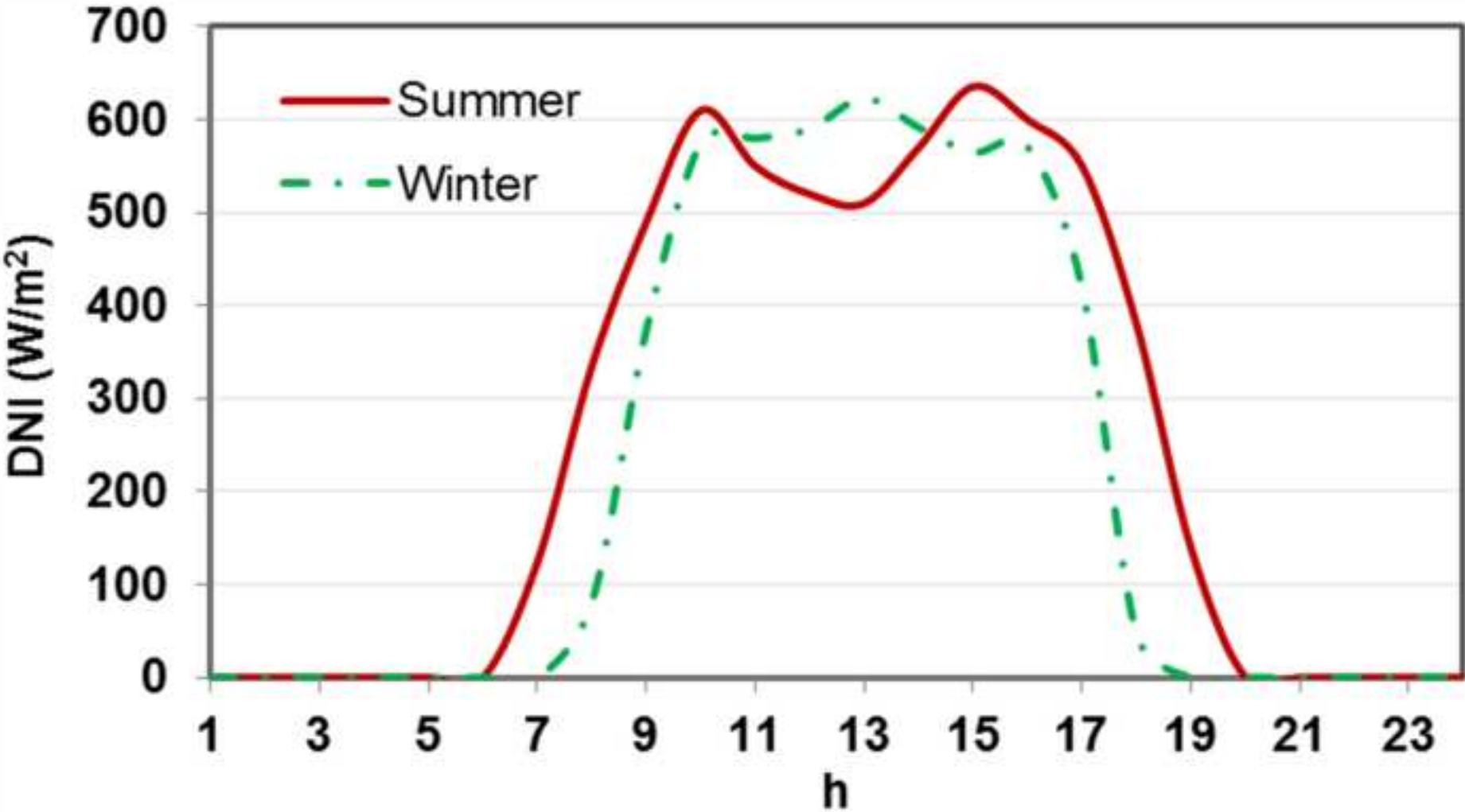


Figure12

[Click here to download high resolution image](#)

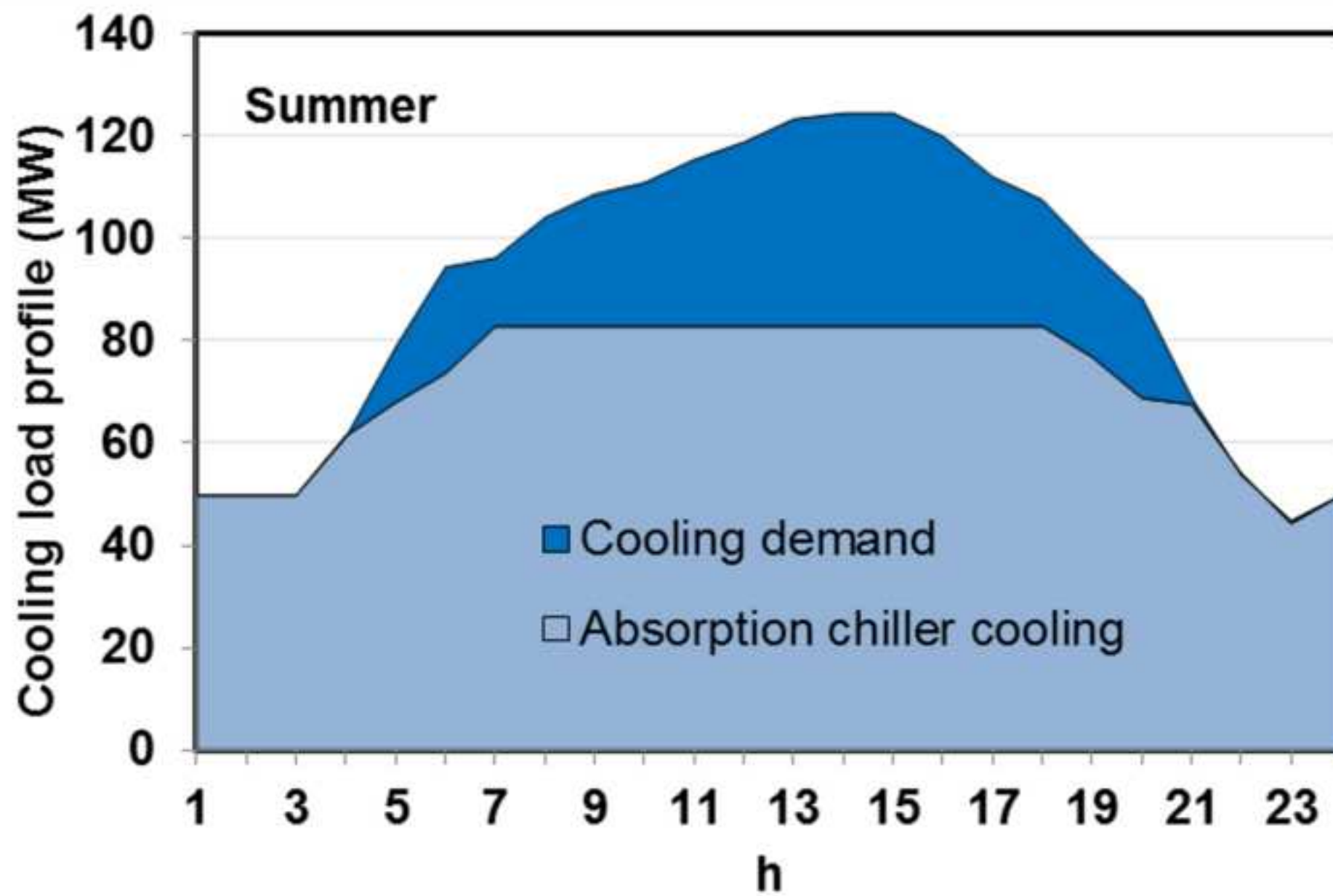


Figure13

[Click here to download high resolution image](#)

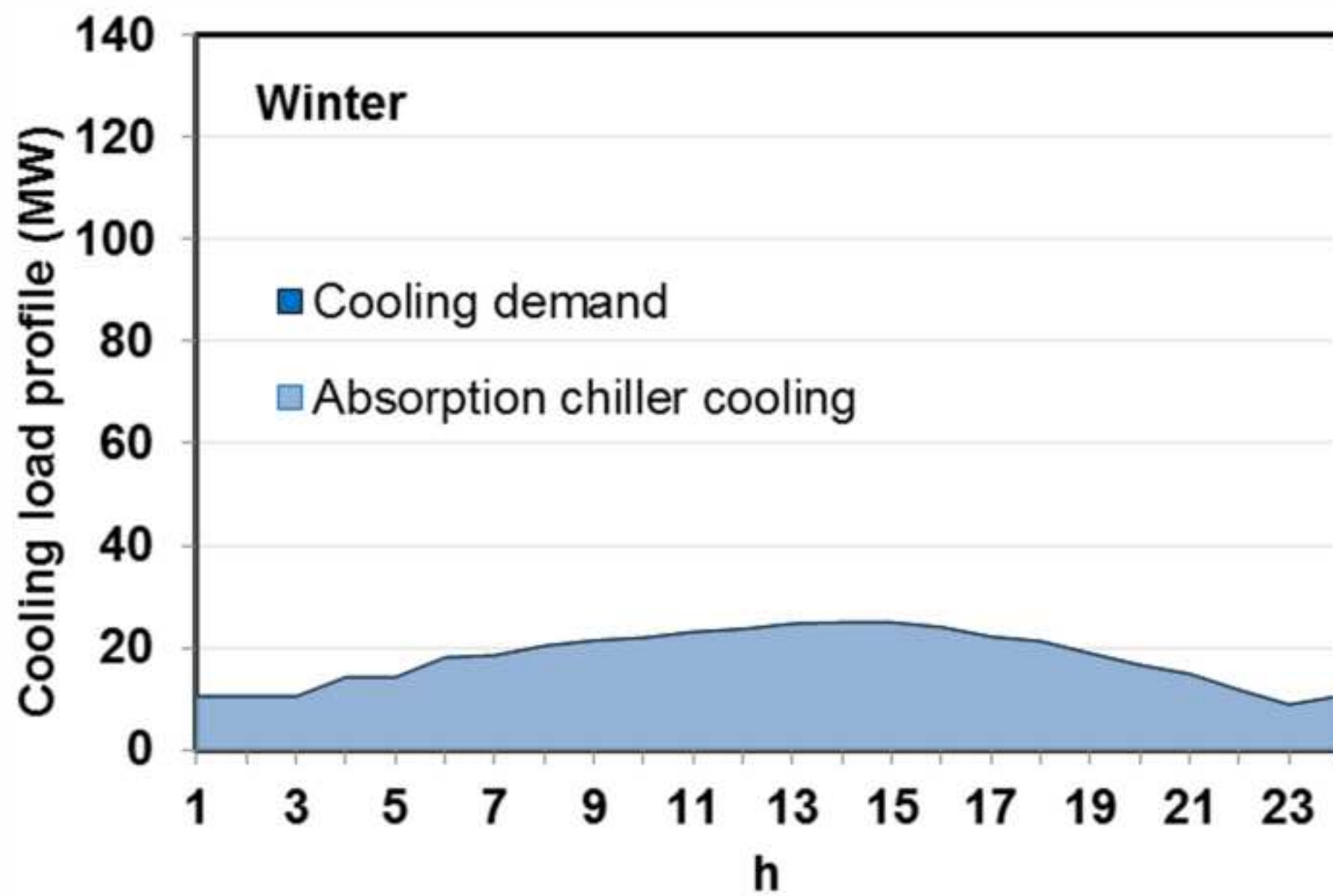


Figure14

[Click here to download high resolution image](#)

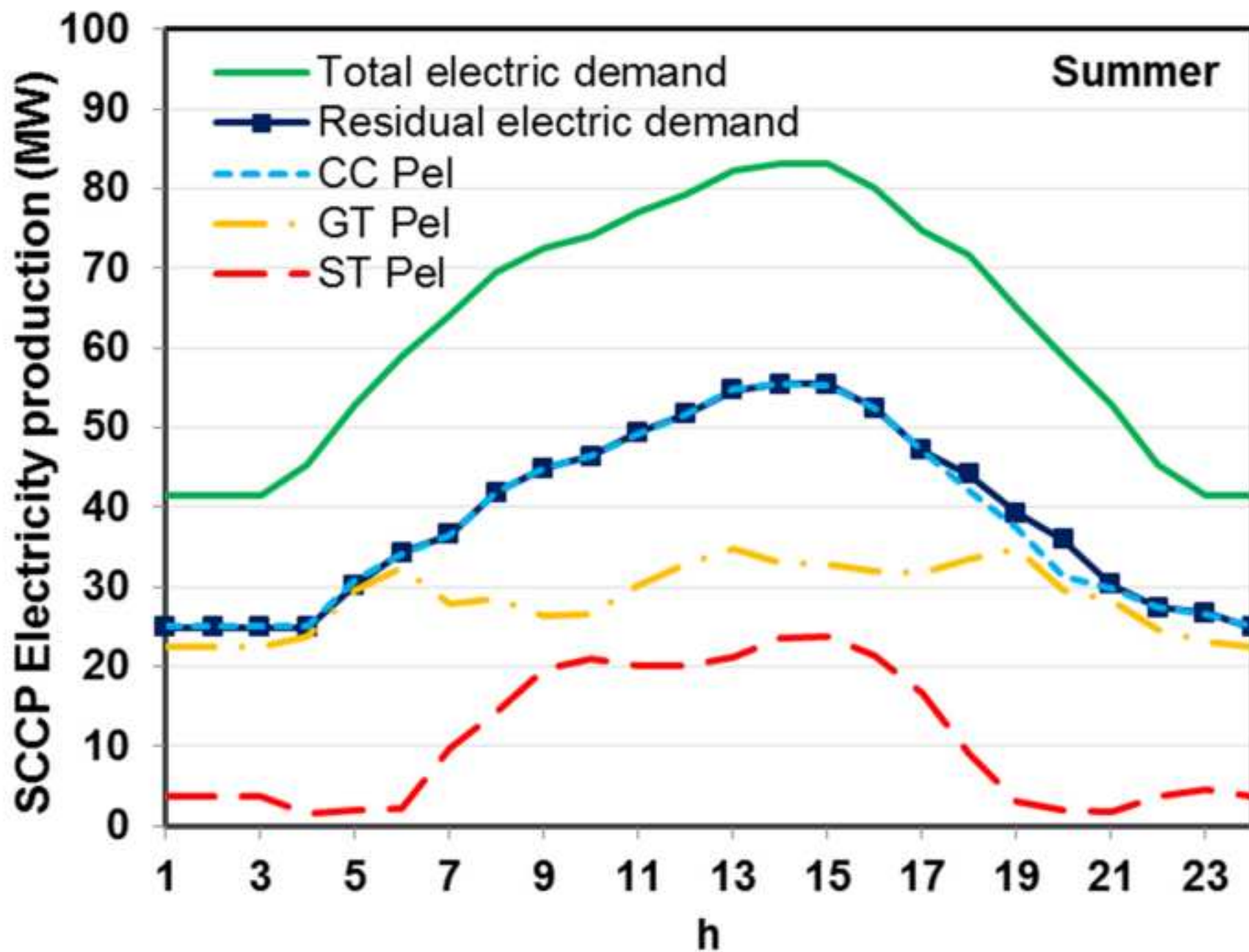


Figure15

[Click here to download high resolution image](#)

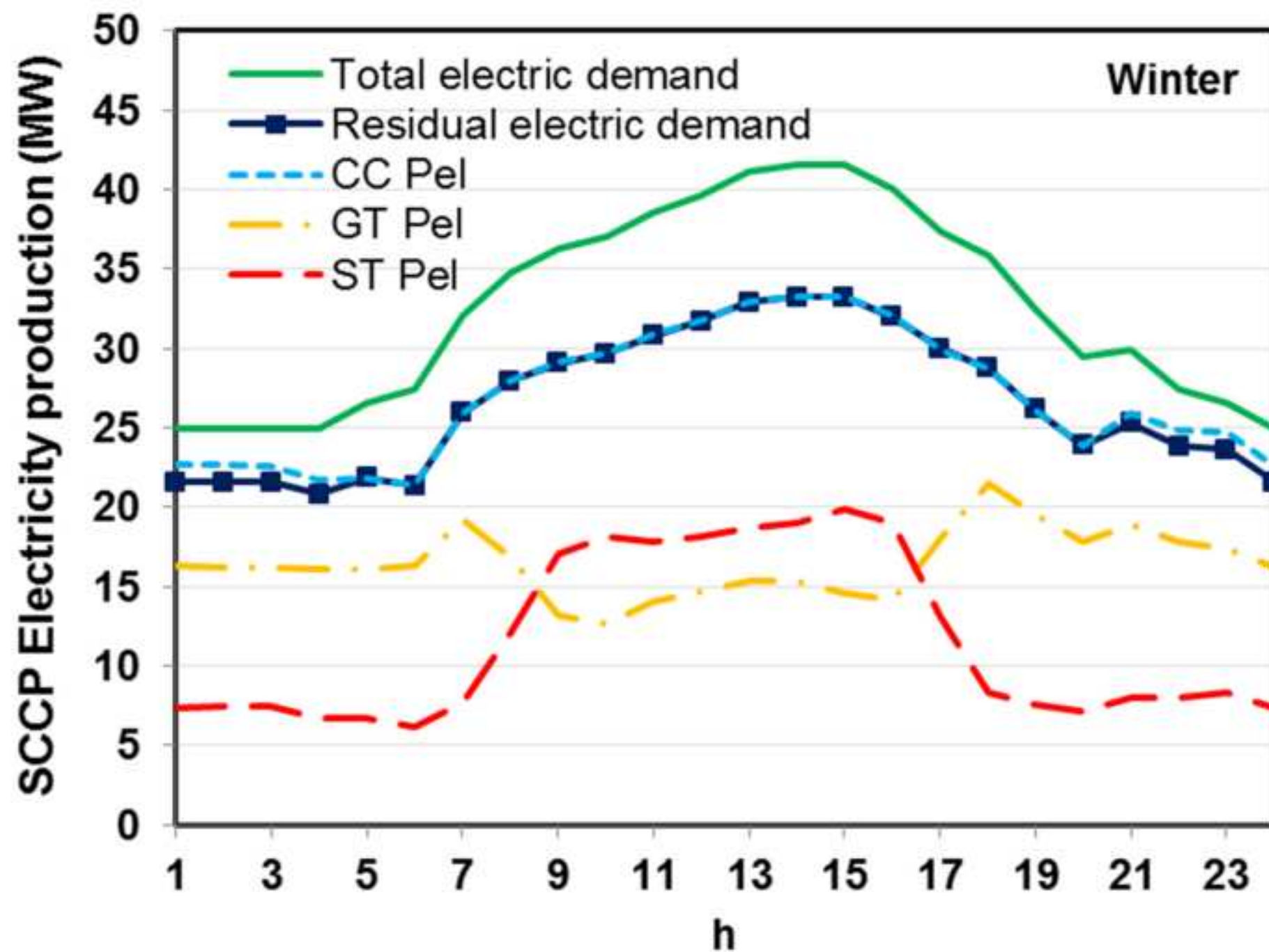


Figure16

[Click here to download high resolution image](#)

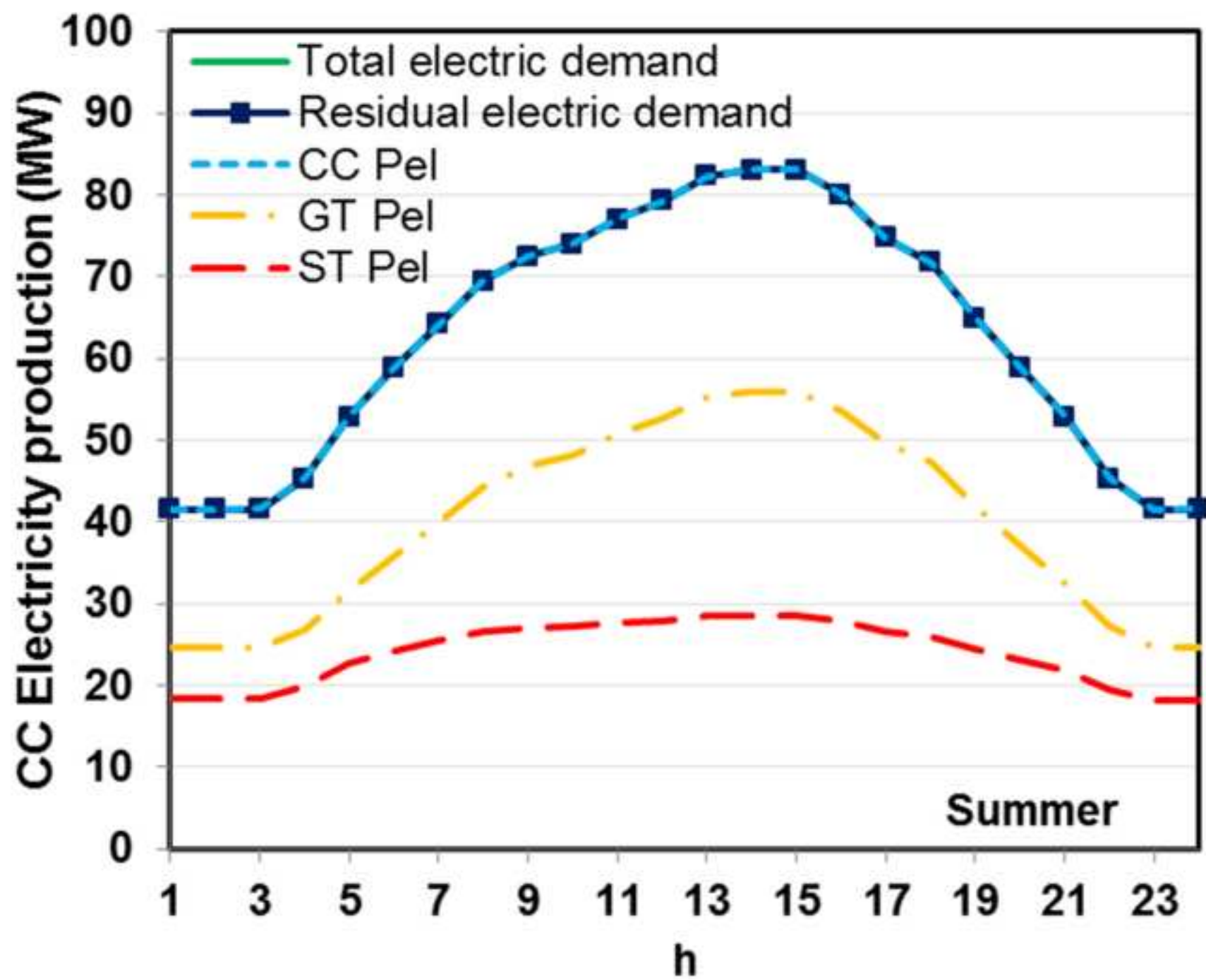


Figure17
[Click here to download high resolution image](#)

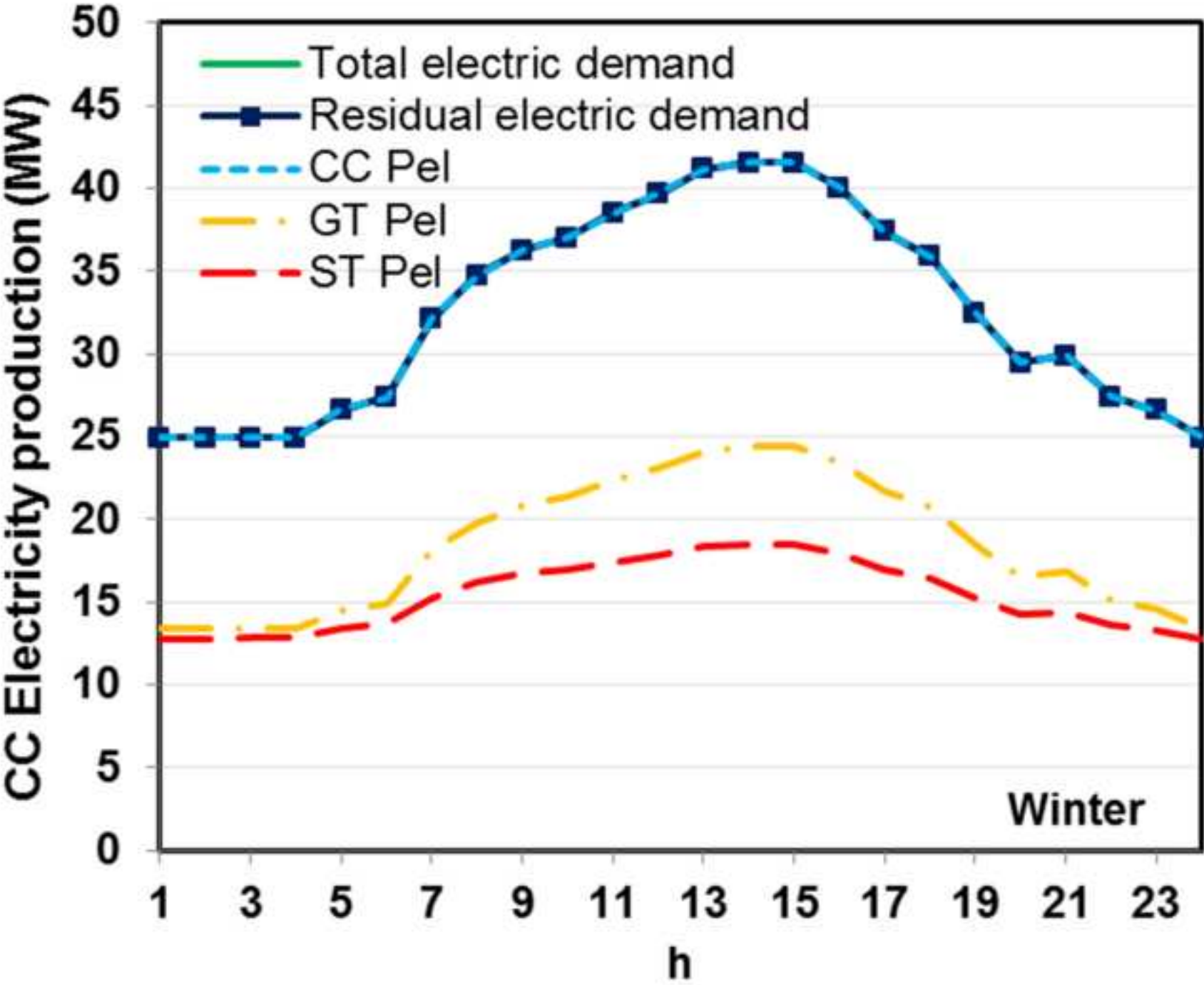


Figure18

[Click here to download high resolution image](#)

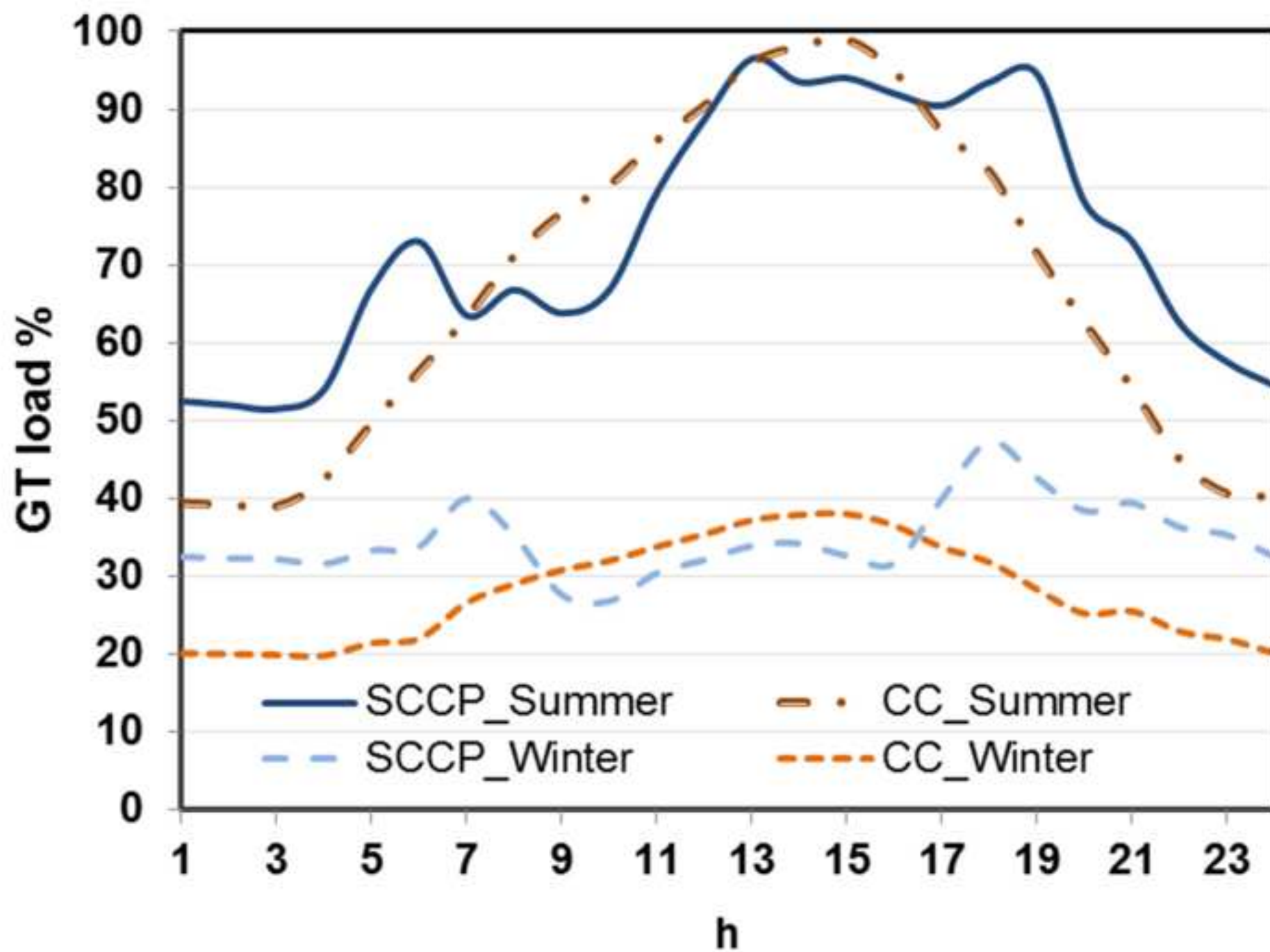


Figure19
[Click here to download high resolution image](#)

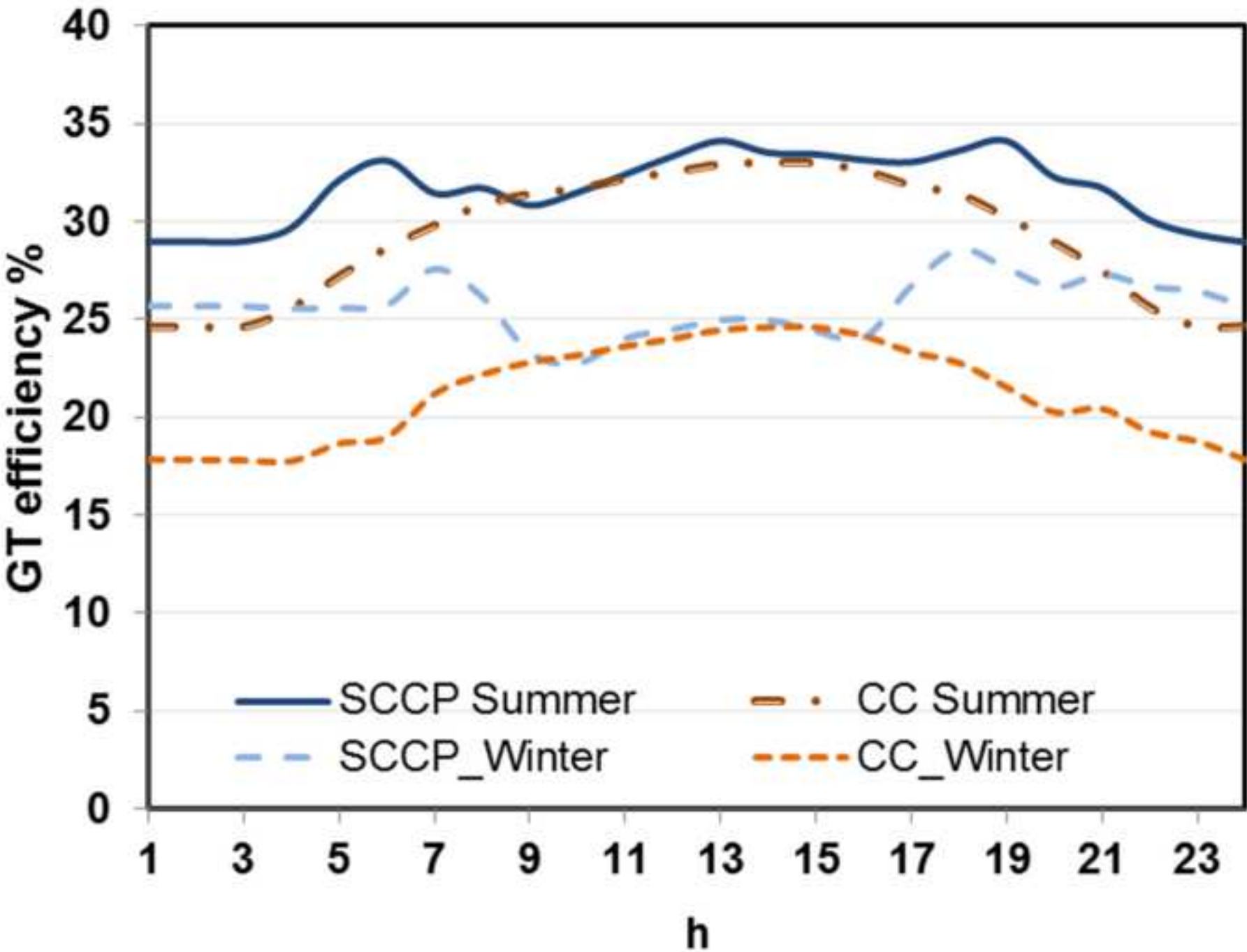


Figure20
[Click here to download high resolution image](#)

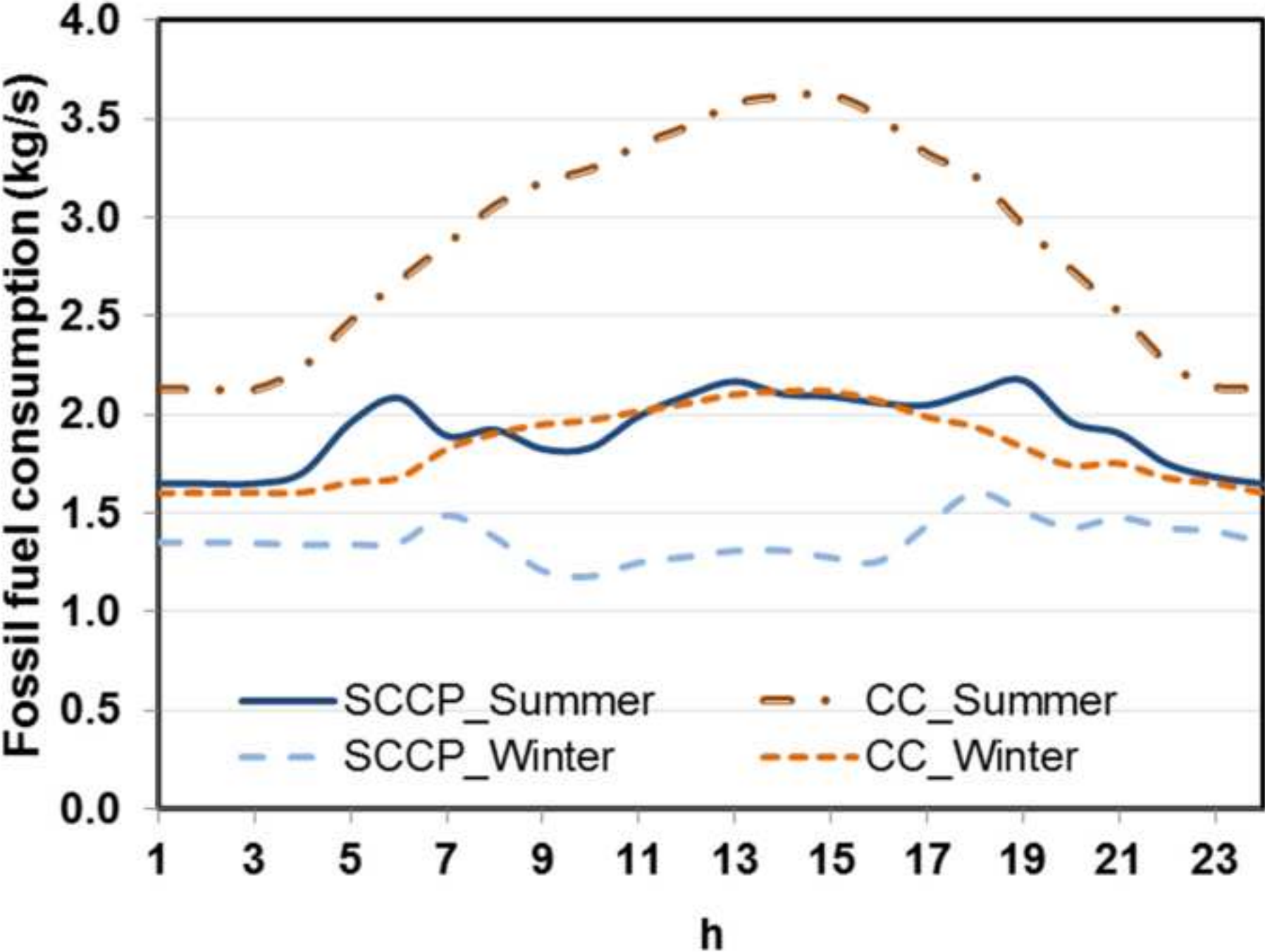


Figure21
[Click here to download high resolution image](#)

